AD-A187 223 INJECTION PROCESSES IN LIQUID REGENERATIVE PROPELLANT GUNS(U) ARMY BALLISTIC RESEARCH LAB ABERDEEN PROVING GROUND MD T P COFFEE AUG 87 BRL-TR-2846

1/1

UNCLASSIFIED F/G 19/1 NL

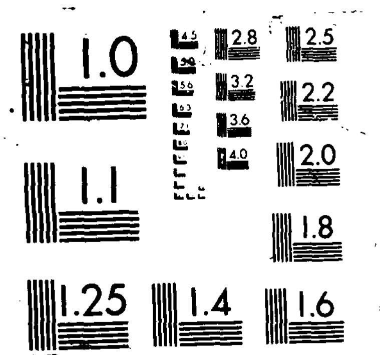
1.0
1.1
1.25
1.4
1.6
1.8
2.0
2.2
2.5
2.8
3.2
3.6
4.0

AD-A187 223

AD

DTIC FILE COPY

TECHNICAL REPORT BRL-TR-2846

INJECTION PROCESSES IN LIQUID REGENERATIVE PROPELLANT GUNS

TERENCE P. COFFEE

AUGUST 1987

US ARMY BALLISTIC RESEARCH LABORATORY
ABERDEEN PROVING GROUND, MARYLAND

UNCLASSIFIED
SECURITY CLASSIFICATION OF THIS PAGE

AD-A187223

REPORT DOCUMENTATION PAGE

Form Approved
OMB No 0704-0188
Exp Date Jun 30, 1986

1a. REPORT SECURITY CLASSIFICATION: Unclassified

1b. RESTRICTIVE MARKINGS

2a. SECURITY CLASSIFICATION AUTHORITY

2b. DECLASSIFICATION / DOWNGRADING SCHEDULE

3. DISTRIBUTION / AVAILABILITY OF REPORT

4. PERFORMING ORGANIZATION REPORT NUMBER(S): BRL-TR-2846

5. MONITORING ORGANIZATION REPORT NUMBER(S)

6a. NAME OF PERFORMING ORGANIZATION: US Army Ballistic Rsch Lab

6b. OFFICE SYMBOL (If applicable): SLCBR-IB

7a. NAME OF MONITORING ORGANIZATION

6c. ADDRESS (City, State, and ZIP Code): Aberdeen Proving Ground, MD 21005-5066

7b. ADDRESS (City, State, and ZIP Code)

8a. NAME OF FUNDING / SPONSORING ORGANIZATION

8b. OFFICE SYMBOL (If applicable)

9. PROCUREMENT INSTRUMENT IDENTIFICATION NUMBER

8c. ADDRESS (City, State, and ZIP Code)

10. SOURCE OF FUNDING NUMBERS

PROGRAM ELEMENT NO	PROJECT NO	TASK NO	WORK UNIT ACCESSION NO

11. TITLE (Include Security Classification): Injection Processes in Liquid Regenerative Propellant Guns

12. PERSONAL AUTHOR(S): Coffee, Terence P.

13a. TYPE OF REPORT: TR

13b. TIME COVERED: FROM ______ TO ______

14. DATE OF REPORT (Year, Month, Day)

15. PAGE COUNT

16. SUPPLEMENTARY NOTATION

17. COSATI CODES

FIELD	GROUP	SUB-GROUP

18. SUBJECT TERMS (Continue on reverse if necessary and identify by block number)
liquid monopropellant; fuel injection; regenerative gun; discharge coefficient; lumped parameter model; droplet burning

19. ABSTRACT (Continue on reverse if necessary and identify by block number)

In a previous report,[1] I discussed the analysis of experimental measurements for a 30mm regenerative liquid propellant gun. Discharge coefficients for the injection into the combustion chamber and values for the Sauter mean diameter of droplets in the combustion chamber were derived. More recently, pressure measurements were also taken in the gun tube. This allows the derivation of discharge coefficients for the flow into the tube. A number of improvements have been made in the inverse analysis. Also, work has been done in developing a transient model to predict the discharge coefficients into the combustion chamber.

20. DISTRIBUTION / AVAILABILITY OF ABSTRACT
☐ UNCLASSIFIED/UNLIMITED ☒ SAME AS RPT ☐ DTIC USERS

21. ABSTRACT SECURITY CLASSIFICATION: Unclassified

22a. NAME OF RESPONSIBLE INDIVIDUAL: Terence P. Coffee

22b. TELEPHONE (Include Area Code): (301) 278-6169

22c. OFFICE SYMBOL: SLCBR-IB-B

DD FORM 1473, 84 MAR

83 APR edition may be used until exhausted
All other editions are obsolete

SECURITY CLASSIFICATION OF THIS PAGE
UNCLASSIFIED

TABLE OF CONTENTS

LIST OF FIGURES

LIST OF FIGURES (CON'T)

I. INTRODUCTION

In this article we consider annular liquid propellant guns (see Figure 1). The regenerative piston surrounds a central rod. As the piston begins to move, it opens up a small annular vent between the piston and the bolt. The bolt is tapered, so the vent opening becomes gradually larger. There is a long straight section where the vent area is constant, and finally a back taper to slow down the piston.

The transducer block (crosshatched area) is mounted on Belleville springs (not shown). A set of pins, going through a spacer, actually connect the block and the springs. When the piston begins to move, it pushes back the liquid and the transducer block. Eventually, the block hits against the spacer. Very little injection takes place before the transducer block stops moving. The springs allow the piston to move past the O-ring and over the front taper in the bolt.

The liquid jet then enters the combustion chamber at high speed. The jet may stay in contact with the center bolt or separate from it. After some delay, the jet breaks up into droplets. The droplets formed may break up further or coalese. The propellant will eventually ignite, and may burn as individual droplets or as an envelope flame. Gas recirculation will further affect the spray combustion. It is possible that the time scale is too short for droplets to form, and the jet may form slugs of liquid or other irregular shapes. Also, there is a crash ring immediately in front of the center bolt. This will effect how the jet breaks up and combusts.

The fluid flows from the combustion chamber into the gun tube. For liquid guns, there is typically a large area change between the chamber and the tube.

Regenerative liquid propellant gun codes[2-5] involve a number of simplifying assumptions. As the codes consider only lumped parameter or at most one-dimensional regions, higher dimensional effects are ignored. Besides this, there are three major areas of uncertainty. First is the injection of the liquid propellant through the piston into the combustion chamber. This is

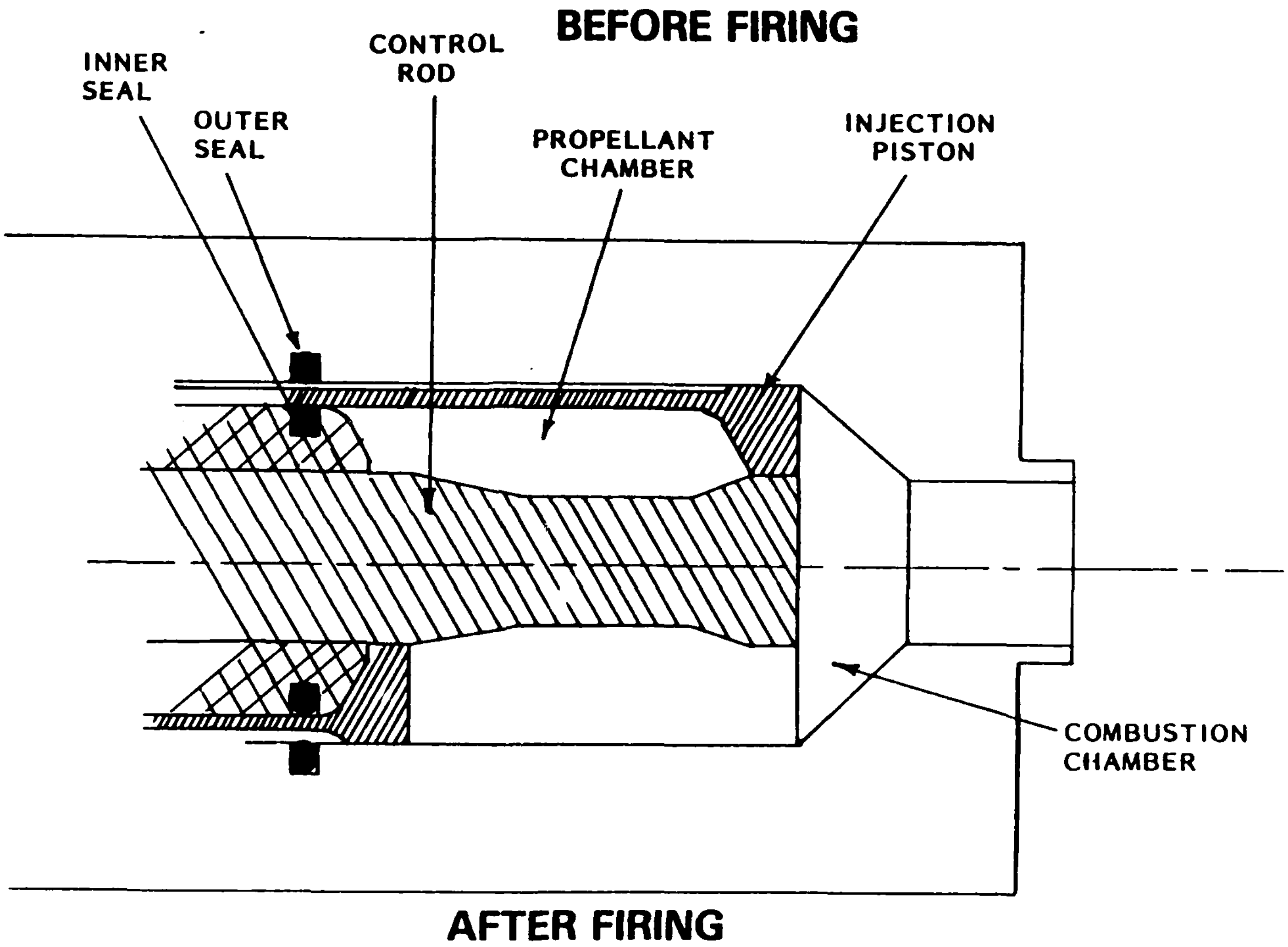

Figure 1. A Regenerative Liquid Propellant Gun with an Annular Piston

approximated as steady state Bernoulli flow. The various possible loss terms (entrance losses, frictional losses, inertial effects, etc.) are lumped into the discharge coefficient. This is treated as an adjustable parameter, and varied so as to obtain the desired chamber pressure.

Second is the liquid accumulation in the combustion chamber. For lack of further information, we usually assume that the liquid combusts instantaneously when it enters the combustion chamber, although simple droplet burning models are also available.

Last, there is the fluid flow from the combustion chamber into the gun tube. This flow is approximated by steady state Bernoulli or isentropic flow, again with an adjustable discharge coefficient to take into account unknown loss terms. This coefficient is normally set equal to one.

At the BRL we have a 30mm regenerative liquid propellant gun.[6] A set of experimental measurements has been made on this fixture.[7] These include the liquid reservoir pressure, the combustion chamber pressure, the piston travel, and the projectile velocity. More recent firings include three pressure measurements in the gun tube (3.81, 50.80, and 241.30 cm. downbore). The pressure traces have been filtered to remove the acoustic oscillations. A number of cases have been measured for the 2/3 charge (about 230 g) and the 1/3 charge. The gun has not yet been fired with a full charge.

The reproducibility of the 1/3 charge firings is not good, so this data is not considered here. We do not have any 2/3 charge cases where all the data was recorded successfully. In this article we consider the data from round 8, where the muzzle pressures were not recorded, and round 53, where the liquid pressure was not successfully recorded. Our goal is to obtain information about the three processes discussed above.

II. NOTATION

In this article, A represents area, E energy, e internal energy, M mass, p pressure, T temperature, V volume, and v velocity. Subscript 1 represents the liquid reservoir, 3 the combustion chamber, and 4 the gun tube. Region 2 (intermediate chamber) does not exist for this fixture. A subscript L represents a liquid property, and a subscript G a gas property. For a complete description, see the List of Symbols.

III. DESCRIPTION OF THE TEXT FIXTURE

Working from the engineering drawings, I have made a scale model drawing of the liquid reservoir (see Figure 2). The combustion chamber side of the piston and bolt have been slightly simplified. The reservoir is initially sealed by an O-ring.

According to the drawings, the transducer block should initially be exactly at the end of the back taper. However, when the test fixture is assembled, the block is observed to be about 1/8 of an inch in front of this point. So the piston stroke, instead of the designed 6.8 cm., is about 6.4 cm. The computed propellant mass is 232 g. A measurement of the propellant needed to fill the reservoir gives a value of 227 g., which is reasonable agreement.[8]

Another measurement[8] shows that the block can move back about 0.5 cm. before hitting a spacer. When the block stops moving, the momentum of the piston causes a rapid pressure rise in the liquid. However, this is observed to occur after the piston has moved approximately 0.6 cm. So I assume that as the block moves back the 0.5 cm, the piston moves 0.6 cm. This causes a small amount of liquid to be injected into the chamber. Figure 3 shows the reservoir after the block has bottomed out. The piston has cleared the O-ring and is over the beginning of the front taper.

The volume of the combustion chamber may be computed. However, a crash ring is inserted into the chamber to protect against damage to the fixture if the piston reverses. This crash ring is complex in shape. So I use a measured value[6] of 95 cc as the initial chamber volume. For the lumped parameter modeling, the volume is the only quantity required. The shape of the combustion chamber is irrelevant.

approximated as steady state Bernoulli flow. The various possible loss terms (entrance losses, frictional losses, inertial effects, etc.) are lumped into the discharge coefficient. This is treated as an adjustable parameter, and varied so as to obtain the desired chamber pressure.

Second is the liquid accumulation in the combustion chamber. For lack of further information, we usually assume that the liquid combusts instantaneously when it enters the combustion chamber, although simple droplet burning models are also available.

Last, there is the fluid flow from the combustion chamber into the gun tube. This flow is approximated by steady state Bernoulli or isentropic flow, again with an adjustable discharge coefficient to take into account unknown loss terms. This coefficient is normally set equal to one.

At the BRL we have a 30mm regenerative liquid propellant gun.[6] A set of experimental measurements has been made on this fixture.[7] These include the liquid reservoir pressure, the combustion chamber pressure, the piston travel, and the projectile velocity. More recent firings include three pressure measurements in the gun tube (3.81, 50.80, and 241.30 cm. downbore). The pressure traces have been filtered to remove the acoustic oscillations. A number of cases have been measured for the 2/3 charge (about 230 g) and the 1/3 charge. The gun has not yet been fired with a full charge.

The reproducibility of the 1/3 charge firings is not good, so this data is not considered here. We do not have any 2/3 charge cases where all the data was recorded successfully. In this article we consider the data from round 8, where the muzzle pressures were not recorded, and round 53, where the liquid pressure was not successfully recorded. Our goal is to obtain information about the three processes discussed above.

II. NOTATION

In this article, A represents area, E energy, e internal energy, M mass, p pressure, T temperature, V volume, and v velocity. Subscript l represents the liquid reservoir, 3 the combustion chamber, and 4 the gun tube. Region 2 (intermediate chamber) does not exist for this fixture. A subscript L represents a liquid property, and a subscript G a gas property. For a complete description, see the List of Symbols.

III. DESCRIPTION OF THE TEXT FIXTURE

Working from the engineering drawings, I have made a scale model drawing of the liquid reservoir (see Figure 2). The combustion chamber side of the piston and bolt have been slightly simplified. The reservoir is initially sealed by an O-ring.

According to the drawings, the transducer block should initially be exactly at the end of the back taper. However, when the test fixture is assembled, the block is observed to be about 1/8 of an inch in front of this point. So the piston stroke, instead of the designed 6.8 cm., is about 6.4 cm. The computed propellant mass is 232 g. A measurement of the propellant needed to fill the reservoir gives a value of 227 g., which is reasonable agreement.[8]

Another measurement[8] shows that the block can move back about 0.5 cm. before hitting a spacer. When the block stops moving, the momentum of the piston causes a rapid pressure rise in the liquid. However, this is observed to occur after the piston has moved approximately 0.6 cm. So I assume that as the block moves back the 0.5 cm, the piston moves 0.6 cm. This causes a small amount of liquid to be injected into the chamber. Figure 3 shows the reservoir after the block has bottomed out. The piston has cleared the O-ring and is over the beginning of the front taper.

The volume of the combustion chamber may be computed. However, a crash ring is inserted into the chamber to protect against damage to the fixture if the piston reverses. This crash ring is complex in shape. So I use a measured value[6] of 95 cc as the initial chamber volume. For the lumped parameter modeling, the volume is the only quantity required. The shape of the combustion chamber is irrelevant.

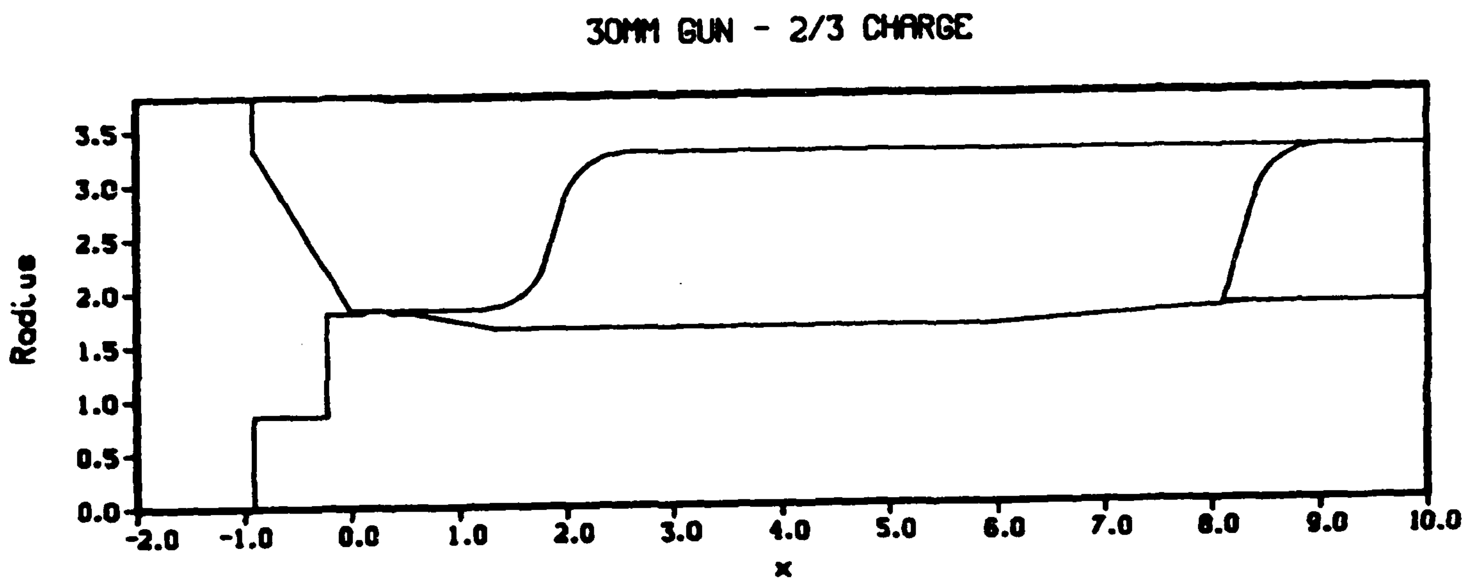

Figure 2. Scale Model Drawing of the Liquid Reservoir (Initial position)

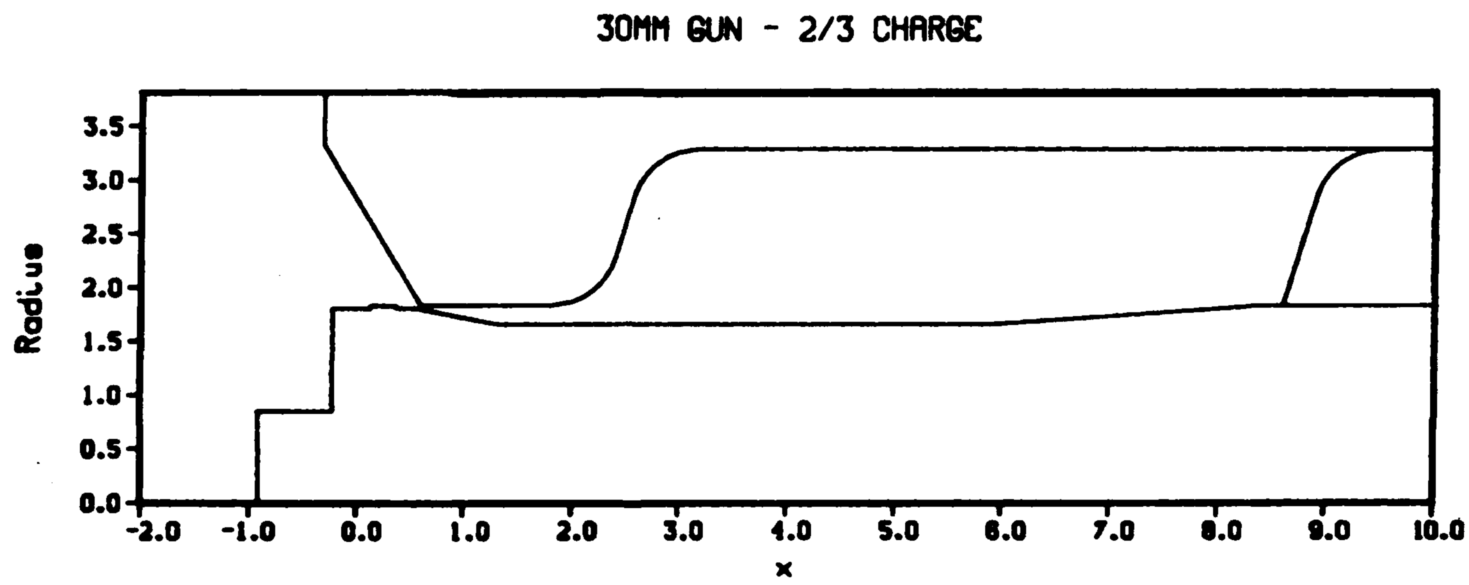

Figure 3. Scale Model Drawing of the Liquid Reservoir (After End of Block Motion)

There is a grease dyke between the piston and the wall of the chamber (except at the front) that helps support the piston. The pressure in the grease is only slightly higher than the combustion chamber pressure during the firing cycle. So in computing the hydraulic difference (combustion side area over liquid side area) the grease area is not included.

Other important numerical values are given in Table 1. Terms are defined in the List of Symbols.

TABLE 1. Fixture measurement.

$A_1 = 33.778$

$A_3 = 45.508$

$A_g = .666$

$A_h = 10.475$

Hydraulic difference $= \dfrac{A_3 - A_h - A_g}{A_1 - A_h} = 1.475$

$S_{max} = 6.436$

V_1 initial $= 162.44$

V_3 initial $= 95.0$

P_1 initial $= 7.0$

P_3 initial $= 17.0$

$M_{ps} = 2138.$

$M_{pj} = 287.1$

The liquid reservoir is pre-pressurized to 7.0 MPa. The primer will pressurize the combustion chamber to about 17 MPa. I do not attempt to model the details of the primer combustion.

IV. PROPELLANT

The propellant used is HAN1846. The relevant properties are given in Table 2.

TABLE 2.

Property	Reference
$\rho_o = 1.43$	9
$e_1 = 4035.5$	9
$\gamma = 1.2226$	9
$c_v = 1.6348$	9
$c_p = 1.9987$	9
$b = .667$	9
$K_1 = 5350.$	10
$K_2 = 9.11$	10
$A = 1.64$	11
$B = .103$	11

The equation of state of the liquid is derived assuming that the fluid is isothermal. The result is

$$\rho_L = \rho_o \left[\frac{K_2}{K_1} p + 1 \right]^{1/K_2} \tag{1}$$

The linear burning rate was measured for a gelled propellant for pressures less than 100 MPa. The form of the equation is

$$\text{linear burning rate} = Ap^{B} \tag{2}$$

The actual burning rate is the surface area times the linear burning rate. There is some evidence that there is a break in the burning rate expression around 100 MPa, and that the exponent becomes much larger. For this paper, I will simply extrapolate the measured rate.

V. EXPERIMENTAL DATA

Figure 4 shows the measured chamber pressure and liquid pressure for round 8. All the data considered has been filtered to remove the high frequency oscillations. The time zero is taken to be the point where the Belleville springs bottom out.

The igniter raises the pressure in the combustion chamber. This moves back the piston, the liquid, and the transducer block. The liquid pressure rises very slowly. At time zero, the block hits, and the momentum of the piston compresses the suddenly trapped liquid. Since the liquid is nearly incompressible, a small volume change leads to a large pressure change. This large pressure accelerates the liquid, and injection causes to pressure to undershoot. The liquid pressure oscillations gradually die out. As the piston nears the end of its stroke, the pressure measurement breaks up.

The piston travel is also measured (Figure 5). I am assuming that the first 0.5 cm of piston travel correspond to the block motion. The last 6.4 cm (taken to be positive) comprise the actual injection stroke. The velocity of the piston will also be required. In the previous paper,[1] I used a finite difference approximation to obtain the velocity. The time difference had to be fairly large because of the noise in the signal. This lead to a loss of resolution. In this paper I fit the data by a parabolic spline. After some

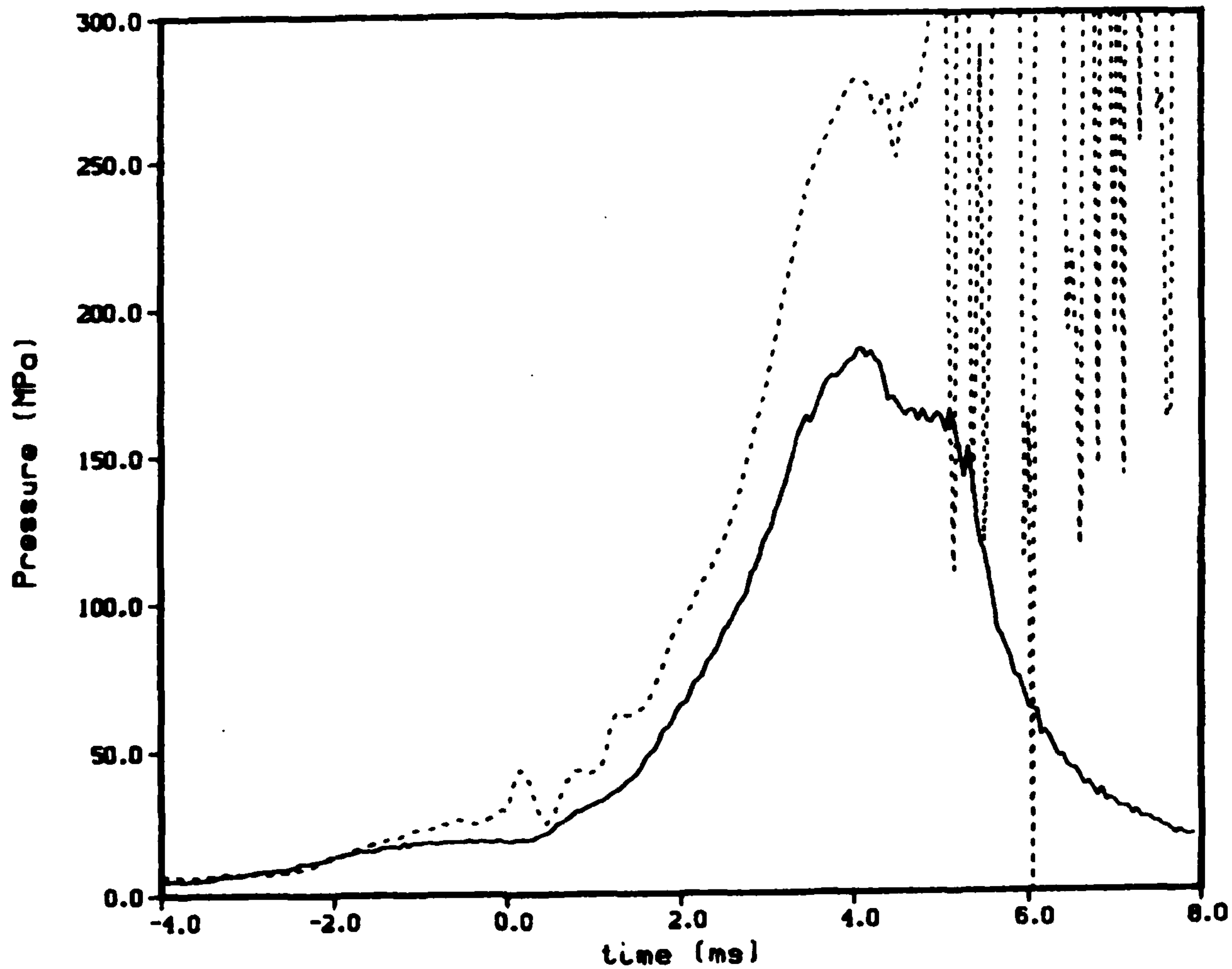

Figure 4. Experimental Chamber Pressure (line) and Liquid Reservoir Pressure (dot); Round 8

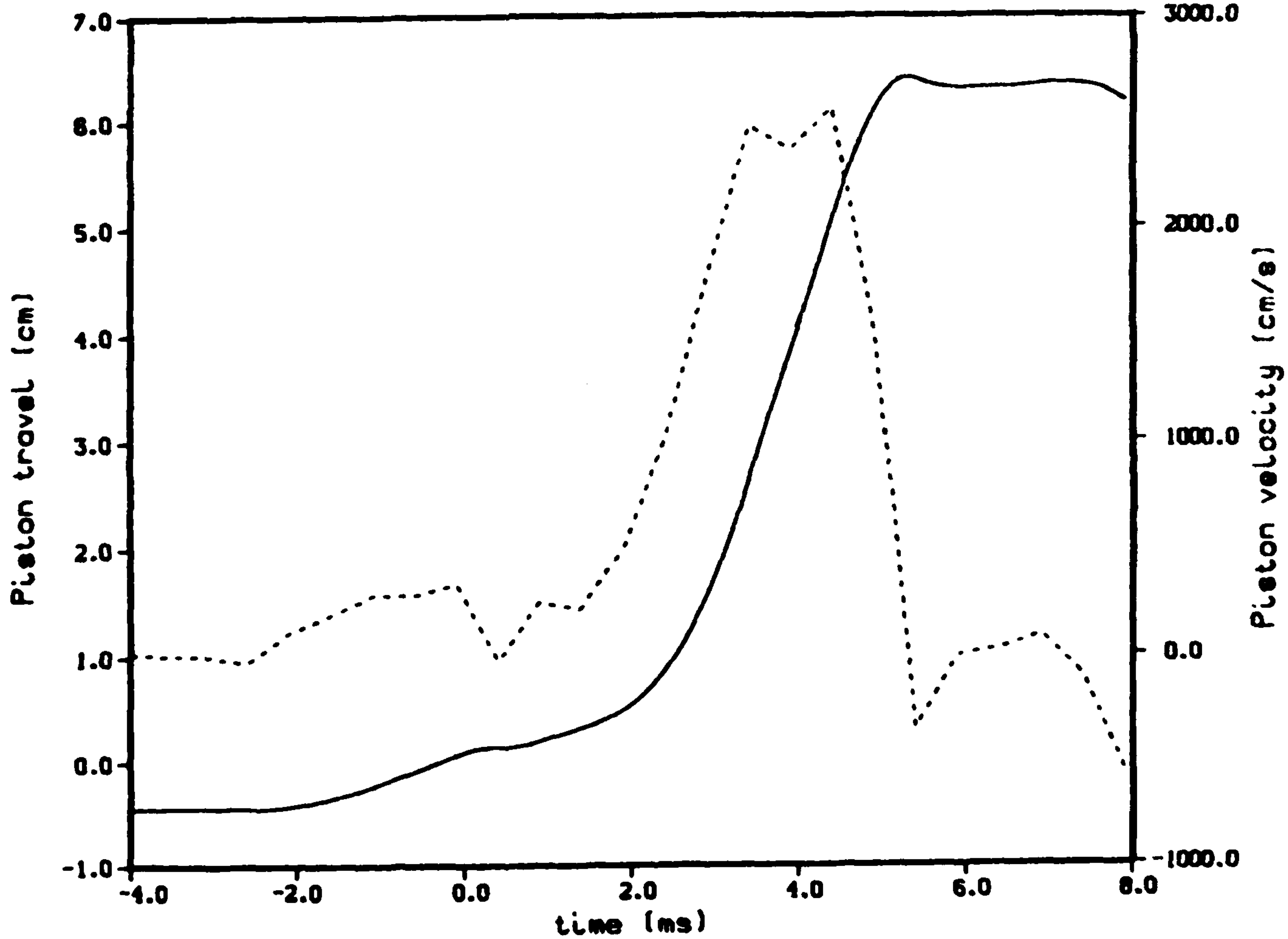

Figure 5. Experimental Piston Travel (line) and Derived Piston Velocity (dot); Round 8

experimentation, I used one parabola for each 0.5 ms. The parabolas are joined at the knots so that the entire curve is continuous and smooth. First and second time derivatives can be taken analytically. Figure 5 also shows the derived piston velocity. This is a linear piecewise function.

For the projectile, the velocity has been recorded using radar. However, this trace is normally accurate only for the middle part of the travel, where the slope of the velocity is fairly constant. To obtain the projectile travel, I fit this section of the curve with two parabolas (see Figure 6). The knot point is where the chamber pressure reaches its maximum. I can then extrapolate in both directions. The projectile travel is now easily obtained by numerical integration.

The projectile has a nominal shot start pressure of 68 MPa. Extrapolating the projectile travel back to zero, I normally obtain a value of shot start pressure between 65 and 70 MPa.

The projectile is seated in the gun tube by hammering. Looking at the raw interferometer data, the projectile seems to move slightly before it is firmly lodged in place. The experimental data is not detailed enough to determine this quantitatively. So I assume that the projectile does not move at all until the pressure reaches 68 MPa.

For Round 8, the gun tube pressures were not recorded. So I also consider Round 53. In this case, the liquid pressure was not successfully recorded, so it is approximated as the chamber pressure times the hydraulic difference. Figure 7 compares the chamber pressures for the two rounds. For Round 53, the spray appears to ignite more rapidly. Also, the behavior near the maximum pressure is quite different. The shape of the pressure curve for Round 8 is more typical.

VI. DATA ANALYSIS

In the gun code, the mass flux through the piston is assumed to obey the steady state Bernoulli l ıw

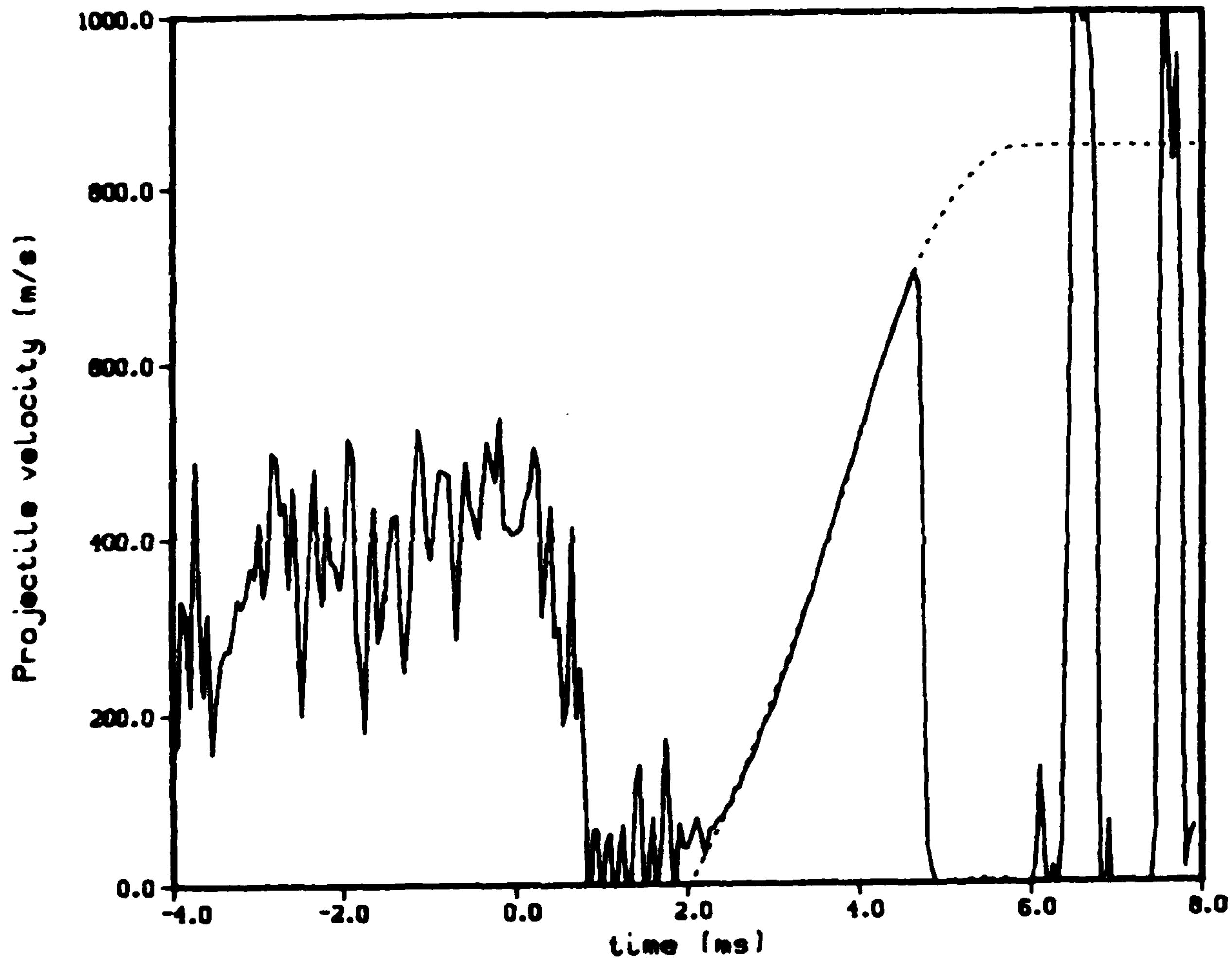

Figure 6. Projectile Velocity; Round 8; Measured (line) and Derived (dot)

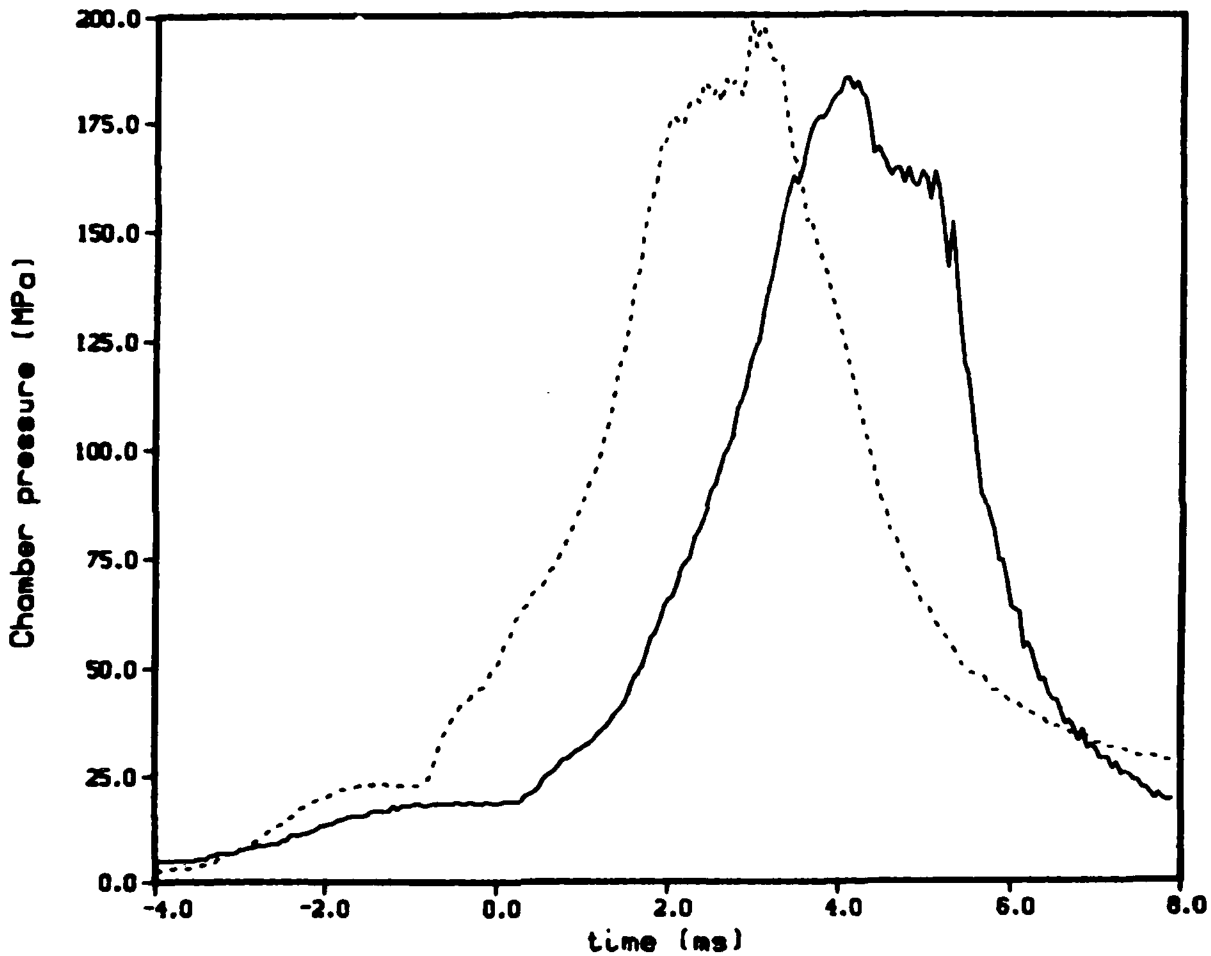

Figure 7. Chamber pressure; Round 8 (line) and Round 53 (dot)

$$\text{mass flux} = C_D A_v \sqrt{2g_o \rho_l (p_l - p_3)} \quad (3)$$

where C_D is the discharge coefficient, A_v is the vent area, g_o is a conversion constant, ρ_l is the liquid density, p_l is the liquid pressure, and p_3 is the combustion chamber pressure.

From the experiment, the pressures and vent area are known. The liquid density can be computed from the equation of state, and the liquid mass in the reservoir is just density times volume. The liquid reservoir mass is fit by cubic splines. The time derivative of this mass can then be taken analytically, and equals the mass flux into the combustion chamber. The discharge coefficient can now be determined.

Results are given in Figure 8. The values are plotted versus the piston travel to make comparisons easier. The early noise is due to the liquid pressure oscillations from the Belleville springs. The discharge coefficient then increases relatively slowly to a more or less steady value. For Round 53, the discharge coefficient becomes larger. This is due to the differences in the chamber pressures for the two rounds. The curves are similar to the results in the previous BRL report. The changes are due to a more accurate accounting for the motion of the Belleville springs and the more accurate method for approximating time derivatives. Because the problem is transient, the discharge coefficient may be greater than one.

It is also possible to compute the liquid accumulation, using conservation of mass and energy. At any given time, we know how much liquid is still in the reservoir. The balance of the original charge is in the combustion chamber/gun tube. We assume that when the liquid combusts, it immediately releases all of its chemical energy. The total energy in the system must equal the chemical energy in the liquid, the internal energy in the gas, and the kinetic energy of the piston, the projectile, and the gas. Energy loss terms (heat loss to the tube, air shock, frictional resistance, etc.) are ignored.

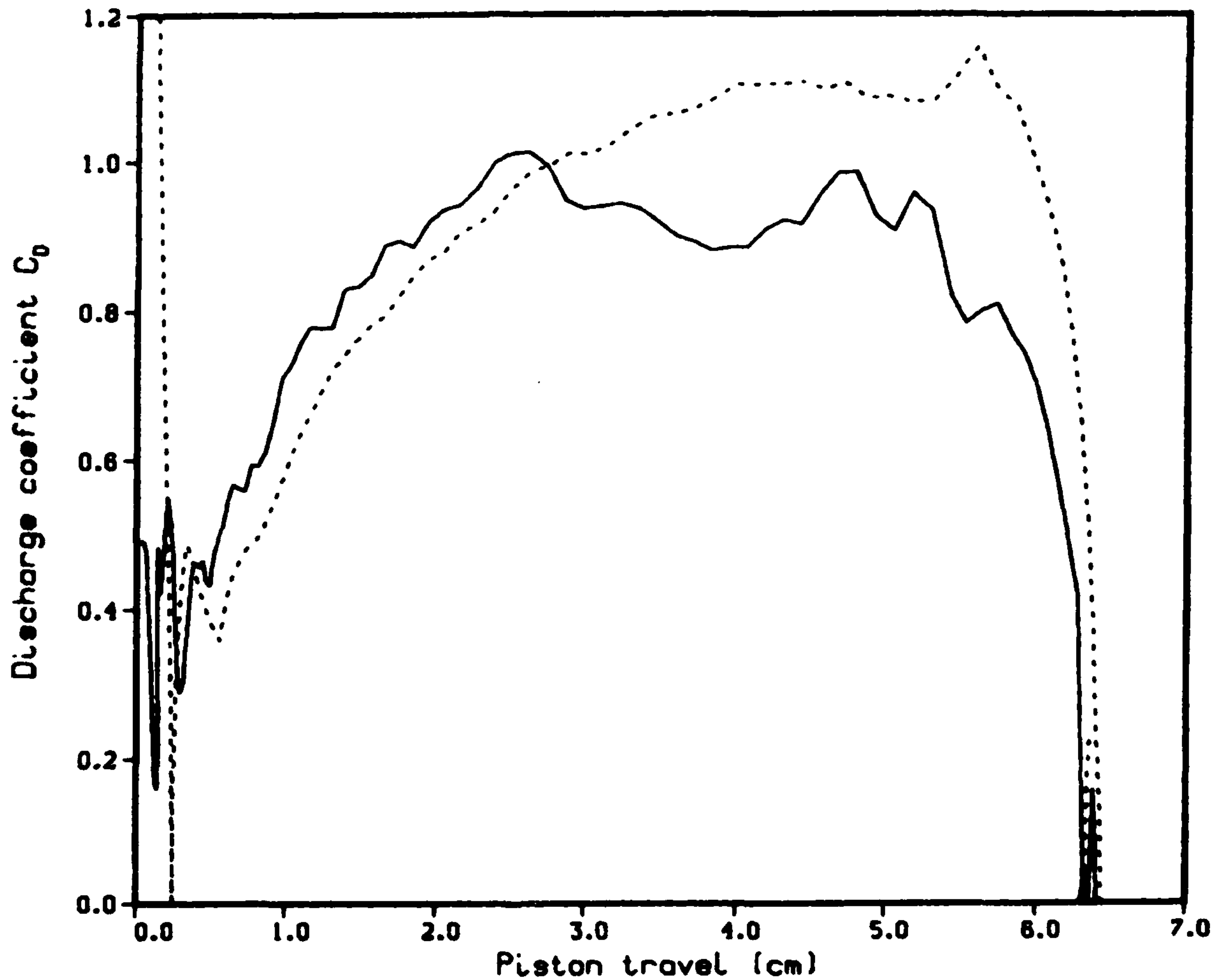

Figure 8. Discharge Coefficient into Combustion Chamber; Round 8 (line) and Round 53 (dot)

The tube pressure is assumed to satisfy a Lagrange pressure distribution. The throat pressure is set equal to the pressure at the first gun tube pressure transducer (3.81 cm from the throat). If the gun tube pressure has not been recorded, I use the chamber pressure.

From the piston travel and projectile travel, the volumes of the combustion chamber and the gun tube are computed. Also, the kinetic energy of the piston, the kinetic energy of the projectile, and the kinetic energy of the fluid in the tube (assuming a Lagrange distribution) can be calculated. The liquid density can be calculated from the equation of state.

We can now set up eleven equations involving the combustion chamber/gun tube; total energy, total mass, volume of chamber and tube, internal energy of the gas (Noble-Abel equation) for chamber and tube, liquid density for chamber and tube, gas density for chamber and tube, and average tube pressure. Unfortunately, there are thirteen unknowns; liquid mass, gas mass, liquid volume, gas volume, gas density, and gas internal energy for both chamber and gun tube, and average tube pressure. Additional assumptions are necessary. I assume that the liquid is evenly distributed in the chamber/tube, and that the internal energy of the gas is the same in the chamber and the gun tube. Details of the equations are in Appendix A.

Results are given in Figure 9. There is a significant liquid accumulation, and large amounts of liquid remain until late in the firing cycle. The results should be accurate at early times. Round 53 shows larger accumulation because the gun tube pressure has been recorded. This pressure is less than the chamber pressure, which I am using for Round 8, and so the gun tube gas has less energy. The above analysis ignores any loss terms (such as heat loss to the gun tube walls), and assumes that the fluid in the combustion chamber is stagnant (no kinetic energy). So there is either significant liquid accumulation, or there are important loss terms not usually taken into account.

One possible source of error is the water purge of the system. Before the liquid reservoir is filled and prepressurized, the system is purged with water. This may contaminate the propellant. For a similar GE test fixture,

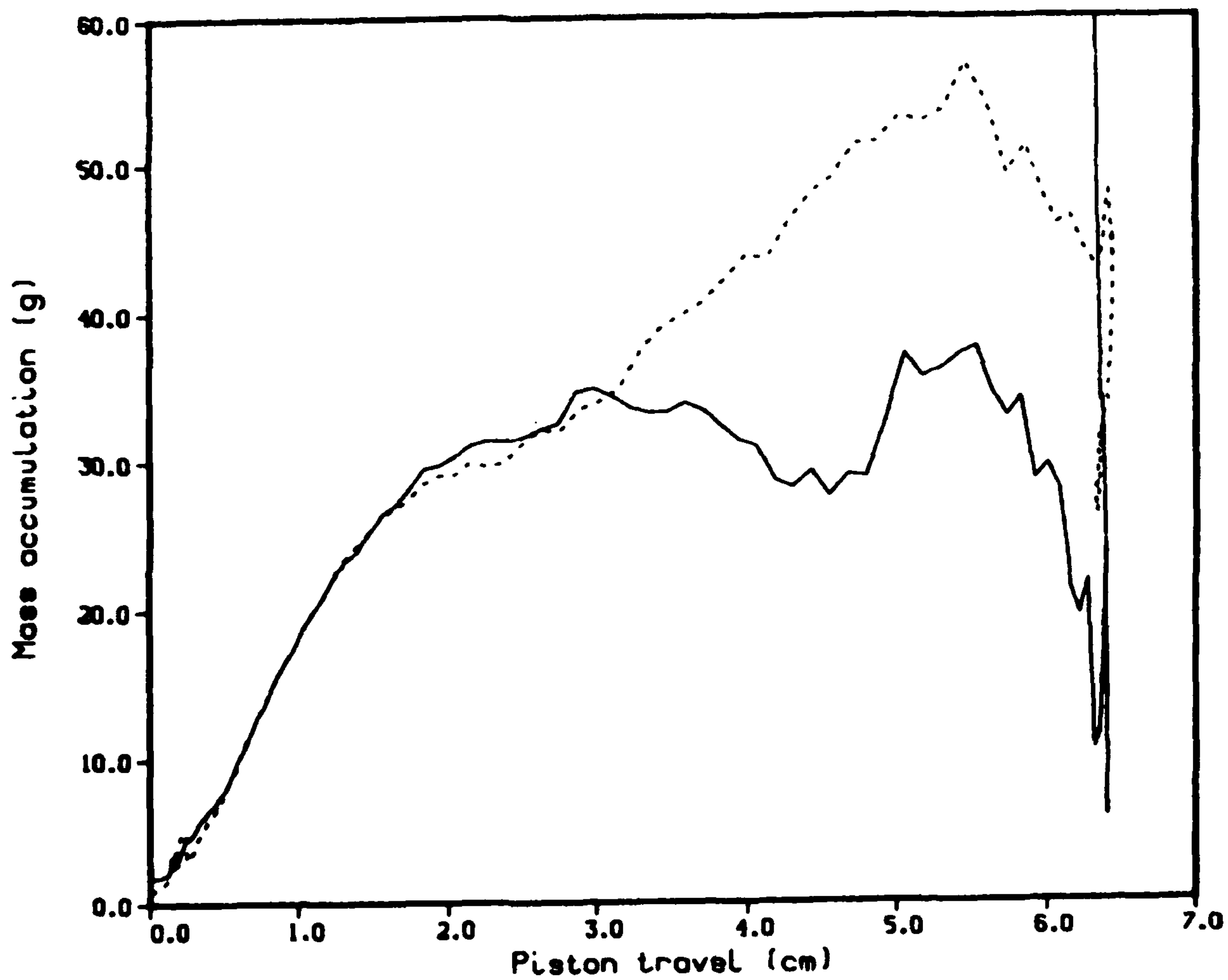

Figure 9. Mass Accumulation in the Combustion Chamber/ Gun Tube; Round 8 (line) and Round 53 (dot)

the liquid in the reservoir is estimated to be as much as 5% water (by volume).[13]

To check on the possible effect of water contamination, I also ran the code assuming 5% water. This was done by changing the initial density of the fluid and its chemical energy. Results are shown in Figure 10. The change is relatively minor.

Heat loss has also been ignored in the above analysis. In gun codes, a heat loss of 5% of the total energy of the system is typical, primarily occuring in the gun tube. This level of heat loss would give results similar to the assumption of 5% water contamination.

Additional information can be obtained concerning the burning rate. Assume that the liquid accumulation is in the form of uniform size droplets. The diameter d_S of the droplets is chosen to be the Sauter mean diameter. This is the diameter that preserves the surface area of the original accumulation. Then

$$\text{burning rate} = M_{L3}\,(6/d_S)\,Ap_3{}^B + M_{L4}\,(6/d_S)\,Ap_4{}^B \qquad (4)$$

where M_{L3} is the liquid in the chamber and M_{L4} is the liquid in the tube. The burning rate is equal to the rate of change of the mass of the gas. Again fitting the total gas mass by splines, the Sauter mean diameter can be calculated (see Figure 11). For early times, the diameter is large, indicating rapid liquid accumulation and slow burning. The diameter then drops rapidly, indicating that the liquid is burning much more efficiently. The liquid accumulation still remains high, but this is due to the rapid influx of propellant from the liquid reservoir. The drop diameter increases late in the cycle. This may actually reflect less efficient combustion, or it may just reflect inaccuracies in the burning rate.

Finally, the mass flux into the gun tube is assumed to be isentropic flow.

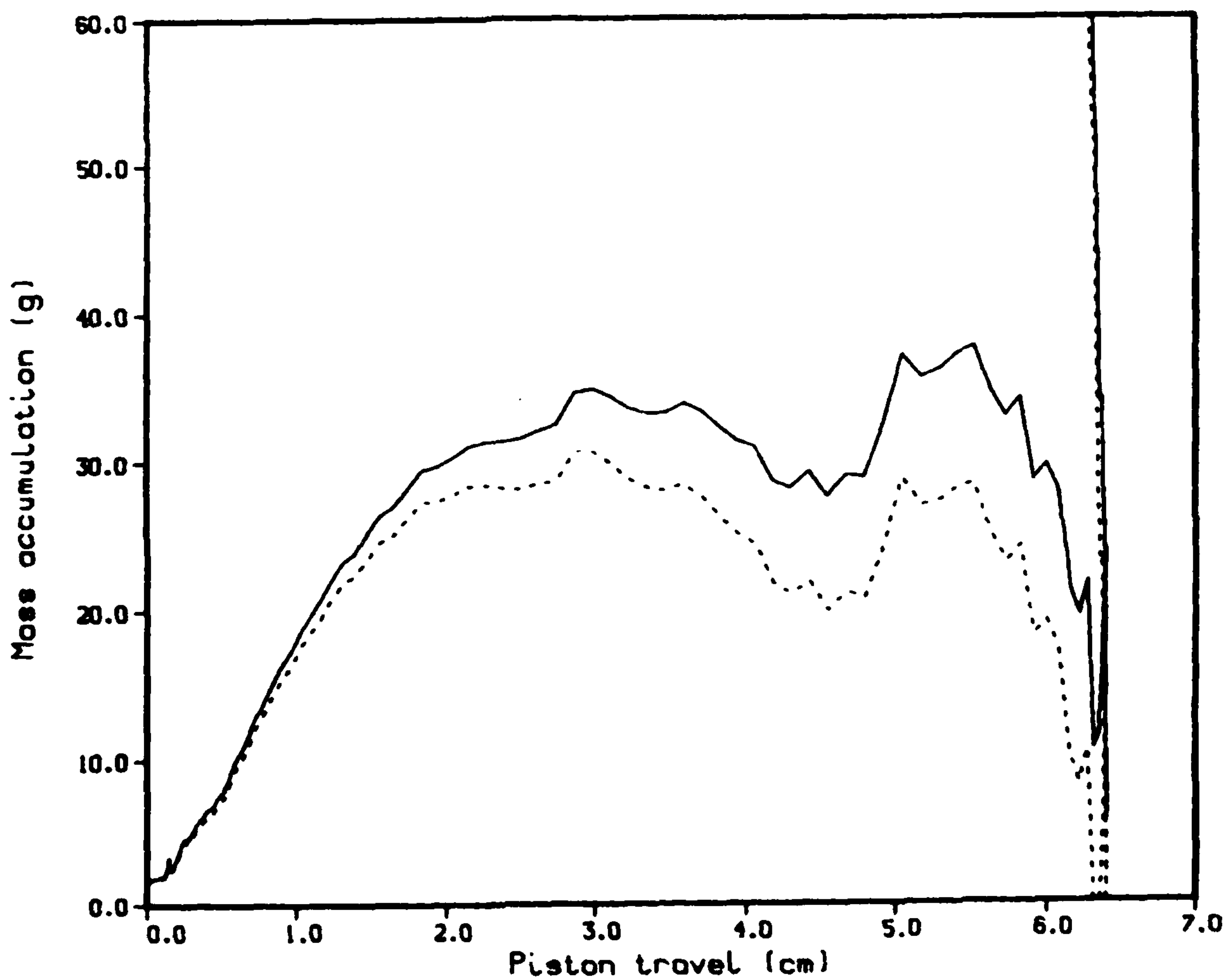

Figure 10. Mass Accumulation in the Combustion Chamber/Gun Tube; Round 8; Pure Propellant (line) and with 5% Water (dot)

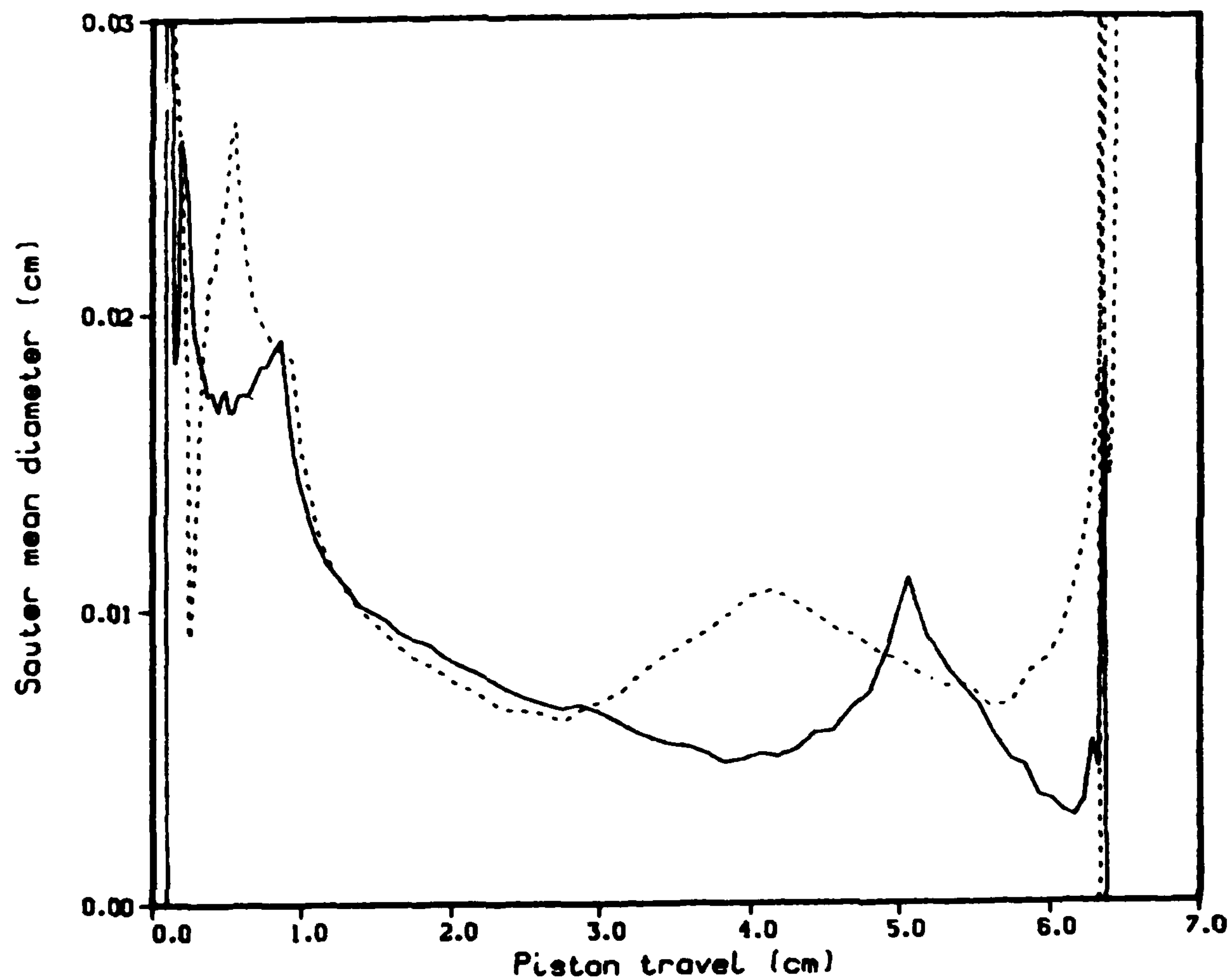

Figure 11. Sauter Mean Diameter of the Liquid Accumulation; Round 8 (line) and Round 53 (dot)

mass flux =

$$C_T A_4 \rho_3 \sqrt{2g_o \{b(p_3 - p_{th}) + c_p T_{th}(p_3/p_4)^{(\gamma-1)/\gamma} - 1]\}} \qquad (5)$$

where C_T is the discharge coefficient, A_4 is the area of the gun tube, b is the covolume of the gas, c_p is the specific heat of the gas, T_{th} is the temperature in the gun tube throat, and γ is the ratio of specific heats. The mass flux is the rate of change of the mass in the tube. So C_T can be computed, and is shown in Figure 12. This result is less accurate than the previous discharge coefficient, since the pressure difference between the chamber and the gun tube is relatively small. If Bernoulli flow is assumed instead of isentropic flow, the results are similar.

VII. COMPARISONS

Now we will see what effect the above results have on our use of the gun code. First the code[5] is run with the usual assumptions. That is, the discharge coefficient is constant with respect to time and the value is chosen to match the desired chamber pressure. The liquid is assumed to burn instantaneously upon entering the combustion chamber (zero liquid accumulation). The discharge coefficient into the gun tube is one. A simple model for air shock and heat loss to the gun tube is included. The pressure distribution in the gun tube is approximated by a modified Lagrange distribution, which takes into account the non-zero fluid velocity at the throat of the tube.

Next, the code is run using the experimental values derived above (for Round 8). The discharge coefficient into the gun tube is read in as a function of piston travel. The liquid injected into the combustion chamber is assumed to form droplets. All the droplets have the same diameter, but this varies with piston travel. Since Round 53 was somewhat different from Round 8, the discharge coefficient into the gun tube will be considered separately. This was only computed for Round 53, and is considered to be less accurate than the other two parameters. For the runs below, this discharge coefficient

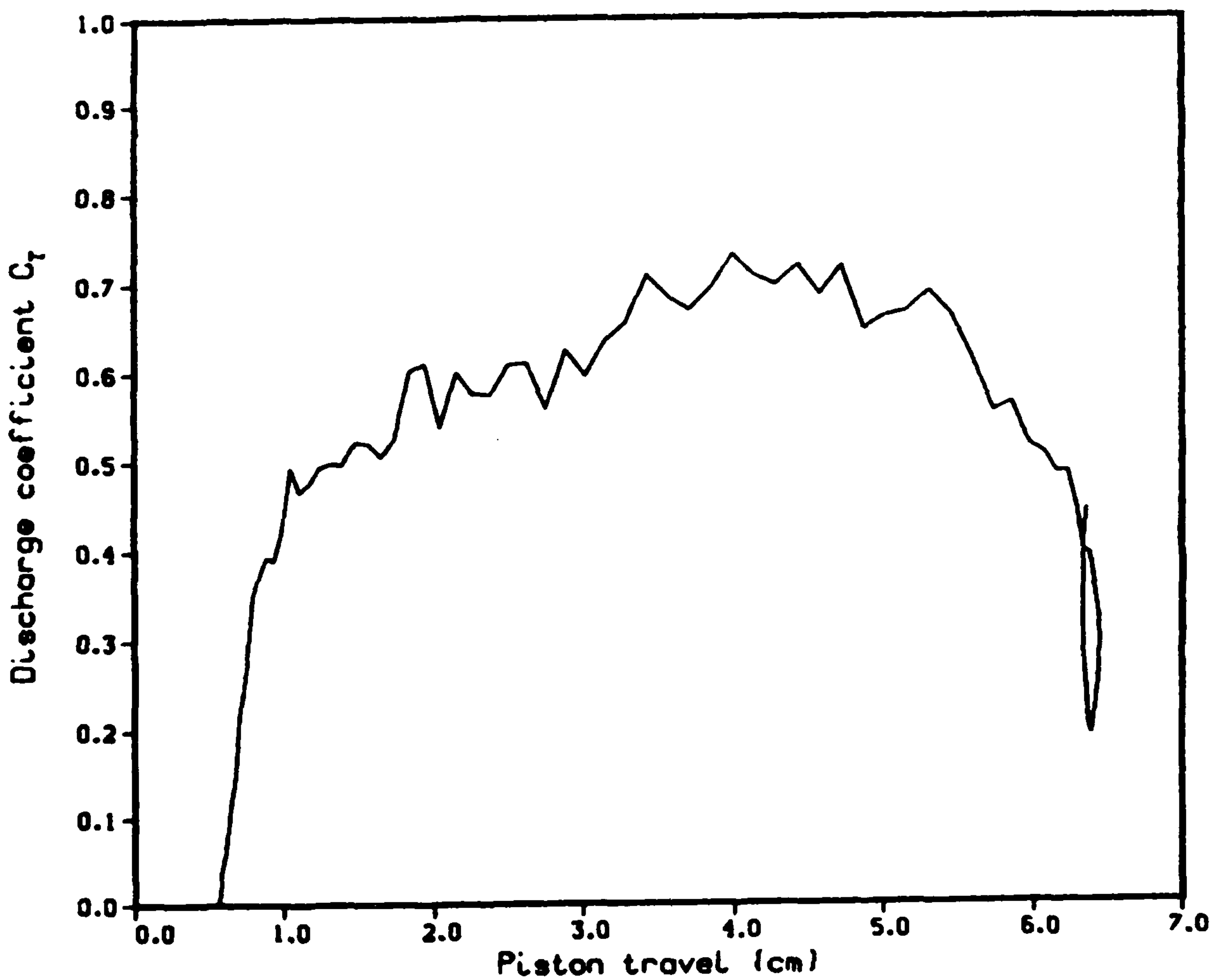

Figure 12. Discharge Coefficient into Gun Tube; Round 53

is set uniformly equal to one. For the purposes of comparison, all the graphs are translated in the time direction so that the chamber pressures reach the shot start pressure (68 MPa) at the same time.

The results for chamber pressure are given in Figure 13. The model using the experimental values reproduces the shape of the pressure curve reasonably well. It it less accurate at early times, since there is no Belleville spring model or primer combustion model in the gun code. It is also less accurate at very late times, when the inverse code is less accurate. The maximum chamber pressure is slightly off, but there was no attempt made to vary the parameters to match this pressure. The simpler model shows a much more rapid pressure rise.

Figure 14 shows the piston travel. The simpler model shows the piston moving slower, since the chamber pressure falls off earlier. In fact, the projectile exits the muzzle before all the liquid is injected.

The projectile velocity is given in Figure 15. The more complicated model shows reasonable agreement.

Figure 16 and 17 show the gun tube pressures. The models give a pressure rise that is later in time than the experimental results. In the models, a shot start pressure of 68 MPa is assumed. This appears to be a good estimate, but in practice the projectile moves a short distance before it is seated firmly. The experimental data indicates that the projectile is already at the first pressure transducer (3.81 cm downbore) when the pressure reaches 68 MPa.

The muzzle velocity for the first model is 1010 m/s and for the second is 1099 m/s. The experimental muzzle velocity is between 1000 and 1020 m/s. The higher velocity for the more complicated model reflects the higher chamber pressure. Also, there are probably additional loss terms not included in the model.

I ran the gun code adding the experimental values for the discharge coefficient into the gun tube (Round 53). The only noticeable result was that the maximum chamber pressure rose 12 MPa. The gun tube pressures and

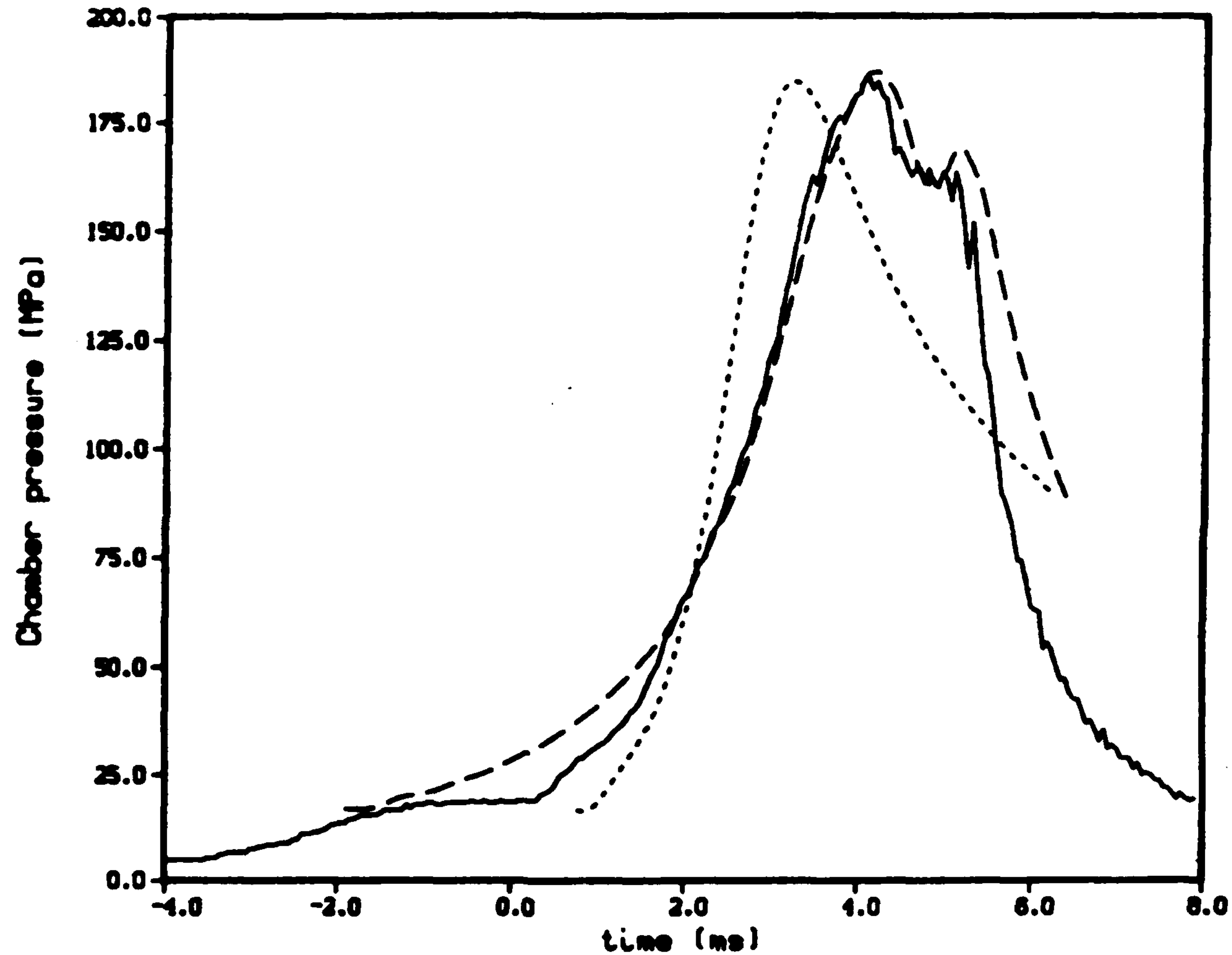

Figure 13. Chamber Pressure for Round 8 (line). Model - C_D=0.59 and Instantaneous burning (dot). Model - C_D and d_s from Round 8 (dash)

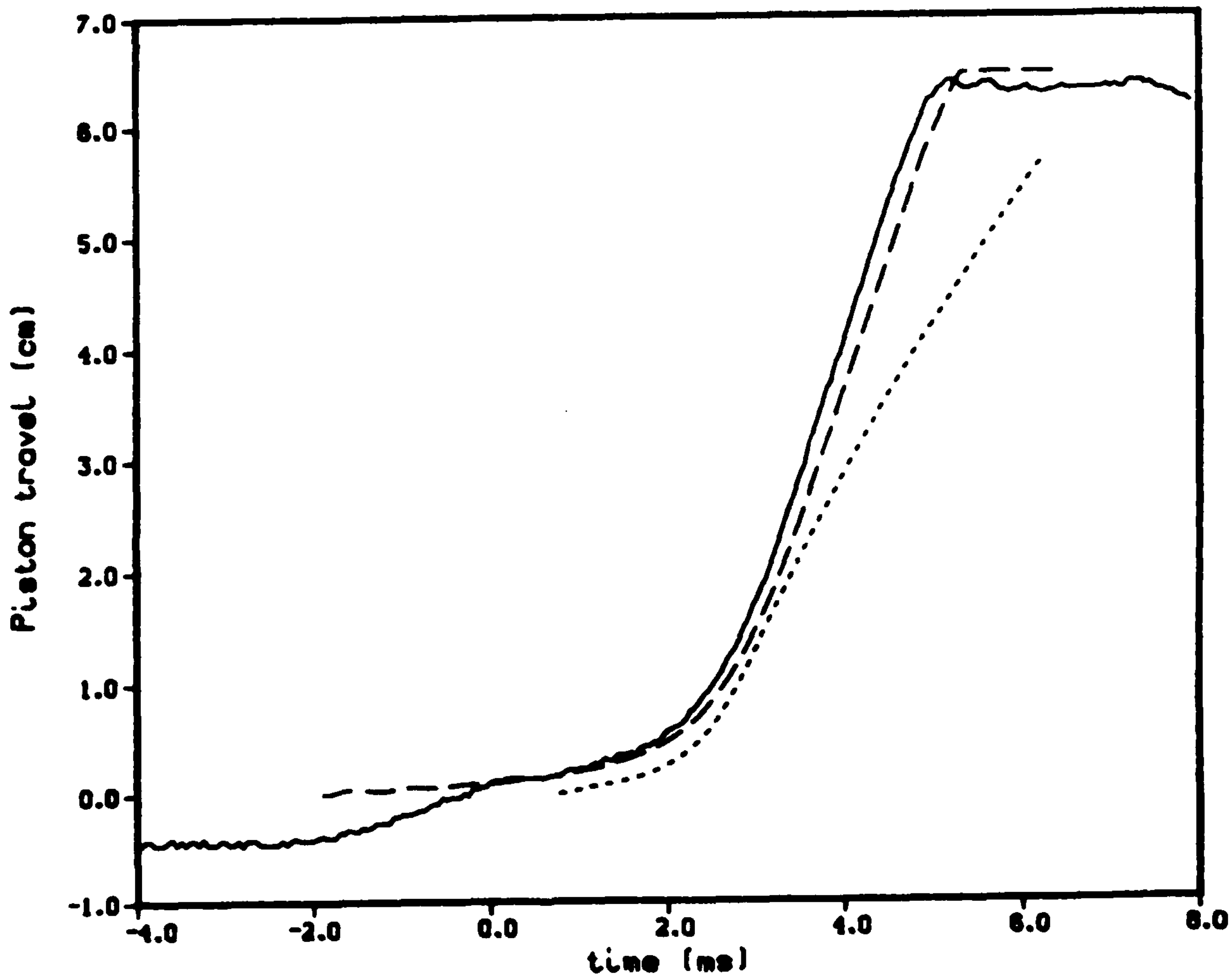

Figure 14. Piston Travel for Round 8 (line). Model - C_D=0.59 and Instantaneous burning (dot). Model - C_D and d_s from Round 8 (dash)

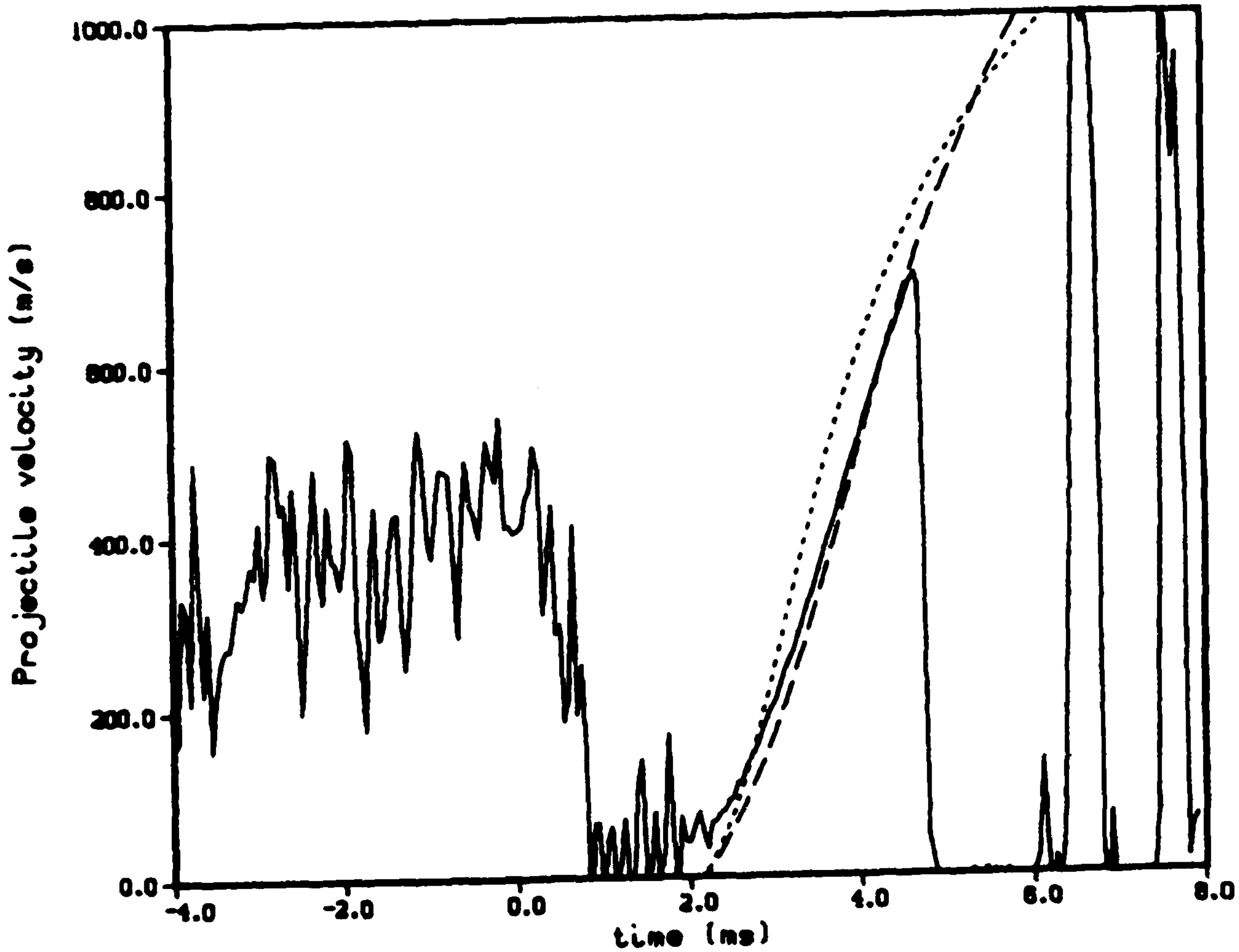

Figure 15. Projectile Velocity for Round 8 (line). Model - C_D=0.59 and Instantaneous burning (dot). Model - C_D and d_S from Round 8 (dash)

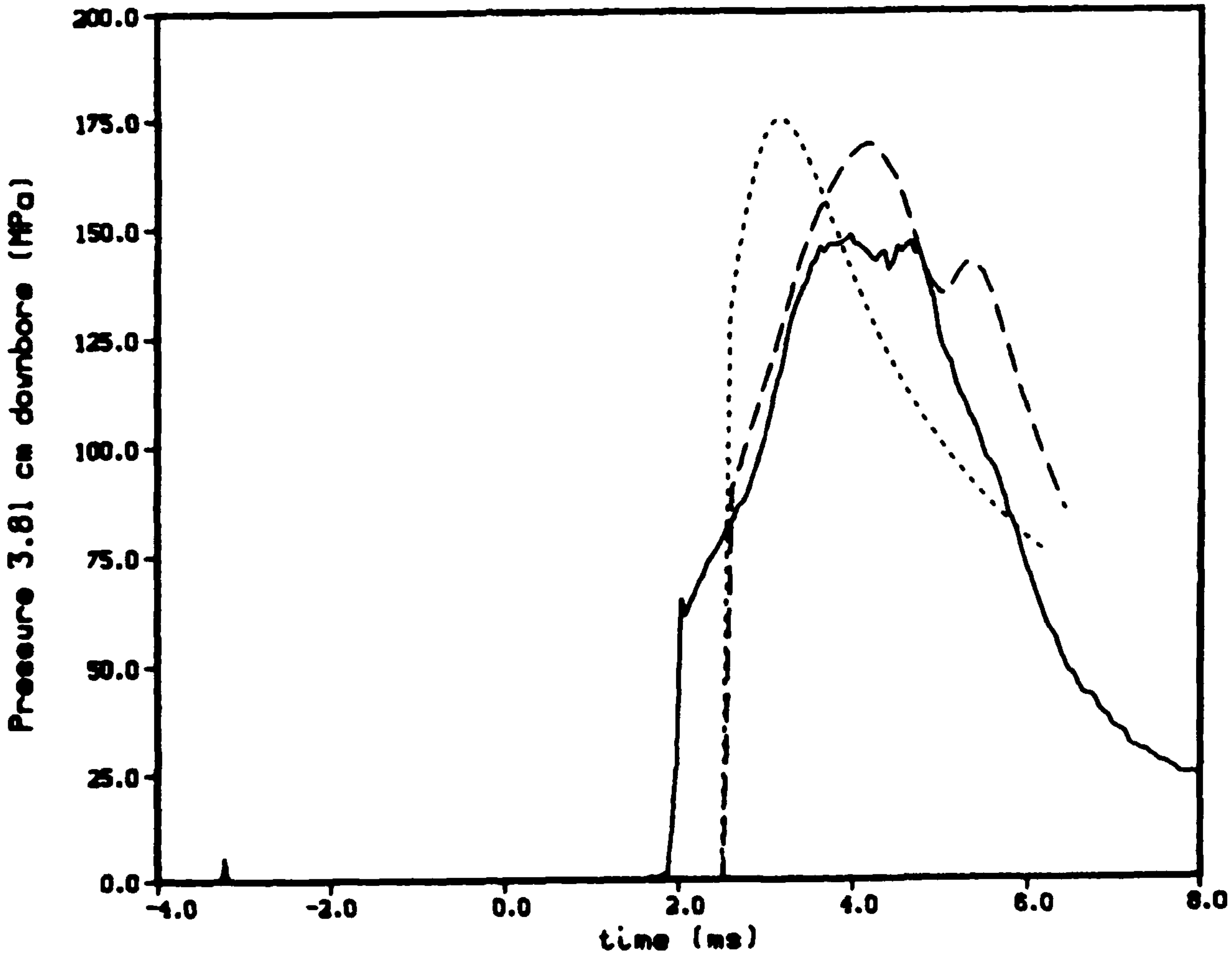

Figure 16. Gun Tube Pressure (3.81 cm Downbore) for Round 53 (line). Model - C_D=0.59 and Instantaneous burning (dot). Model - C_D and d_S from Round 8 (dash)

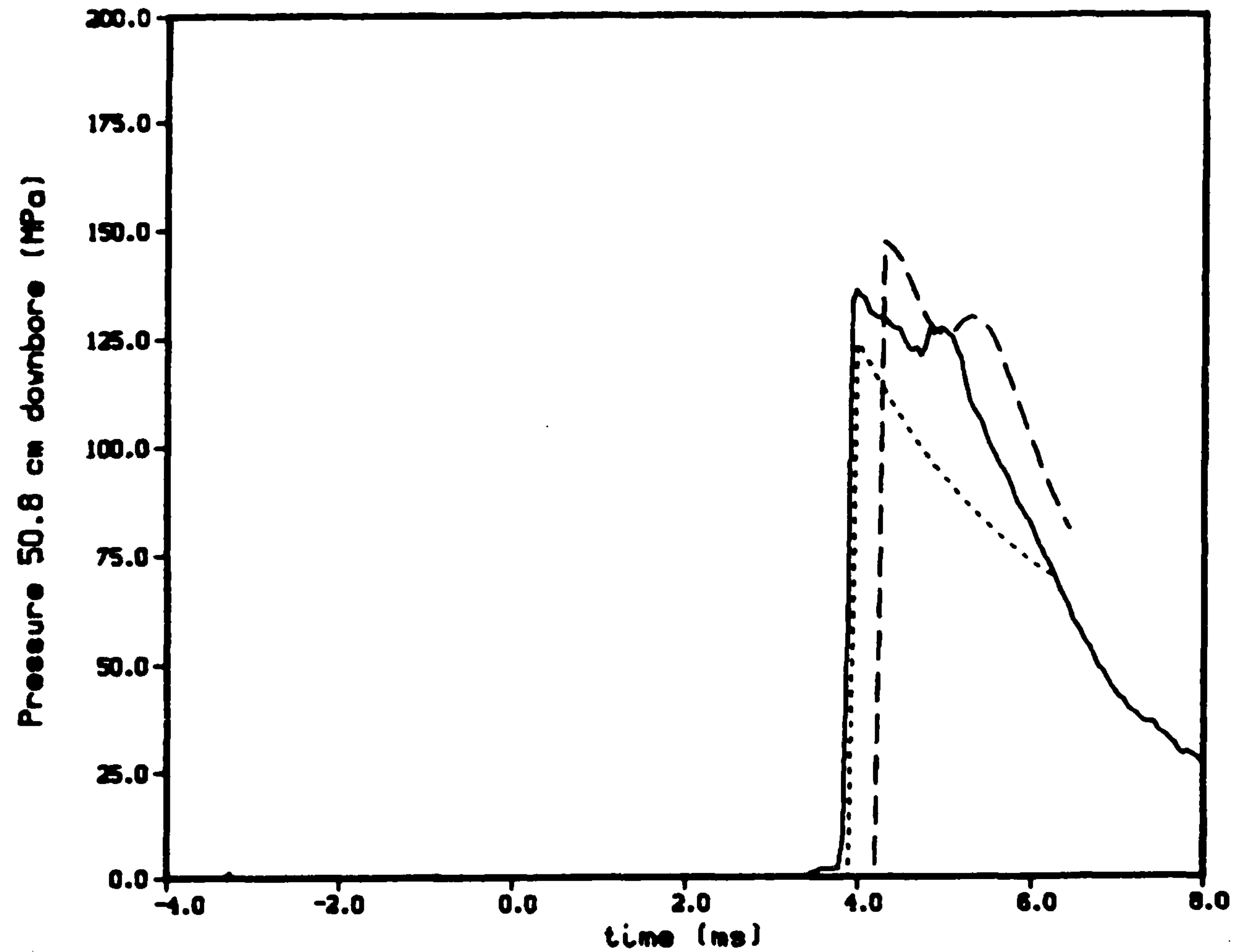

Figure 17. Gun Tube Pressure (50.8 cm Downbore) for Round 53 (line). Model - C_D=0.59 and Instantaneous burning (dot). Model - C_D and d_S from Round 8 (dash)

projectile velocity were practically unchanged. The injection into the gun tube seems to be controlled primarily by the projectile motion. If a smaller discharge coefficient is chosen, the chamber pressure increases sufficiently to sustain about the same injection rate.

In addition, I ran the gun code using the values derived from Round 53 instead of Round 8. The results were qualitatively very similar. The predicted chamber pressure fell 15 MPa, and the second peak in the chamber pressure curve was flattened out. The predicted muzzle velocity decreased by 28 m/s.

VIII. TRANSIENT INJECTION MODELS

It seems reasonable to try to explain the discharge coefficients as due to transient behavior. This involves setting up an unsteady equation for the mass flux.

I assume that the flow in the liquid reservoir is isothermal. In conservation form, the quasi two-dimensional mass and momentum equations are

$$\frac{\partial(\rho A)}{\partial t} = - \frac{\partial}{\partial x} (\rho v A) \tag{6}$$

$$\frac{\partial(\rho v A)}{\partial t} = - \frac{\partial}{\partial x} (\rho v^2 A) - g_o A \frac{\partial p}{\partial x} \tag{7}$$

where v is the liquid velocity and A is the cross sectional area. The coordinate system is fixed with respect to the piston. This is convenient since the division between the liquid reservoir and the combustion chamber is defined by the front corner of the piston. I want to approximate the momentum equation while retaining the simple lumped parameter model.

The assumption I make is that the space derivative of the mass flux ρvA is zero. From the experimental data, this gradient is in fact quite small. Then taking the momentum equation, and integrating from the back wall of the liquid reservoir to the orifice exit, one obtains

$$\frac{\partial(\rho vA)}{\partial t} = [0.5 \ \rho_1 \ (v_{ps}{}^2 - v_3{}^2) + g_o(p_1 - p_3)]/\int dx/A \qquad (8)$$

where v_{ps} is the piston velocity and v_3 is the injection velocity of the fluid. The integral of the inverse of the area is approximated assuming a slightly simplified piston shape.

The above form ignores loss terms. To take this into effect, I multiply the pressure term by a constant discharge coefficient squared.

I implemented this model into the gun code, and ran the code using the experimentally derived Sauter mean diameters and the new transient mass flux model (C_D = 0.958). Given the resulting mass flux, corresponding steady state discharge coefficients can be derived. Figure 18 shows the comparison with the experimental discharge coefficients. While the new model shows the qualitative behavior of a time delay in the rise to steady state discharge coefficients, the rise time is much too rapid.

The difficulty follows from the form of the equations. At the beginning, the mass flux is well below steady state values. Since the liquid cannot be injected through the piston, it is compressed, leading to a rapid pressure rise. But a relatively small pressure difference leads to a very large increase in the mass flux time derivative. Because of this feedback with the piston motion, the approach to steady state is very rapid.

Work is now going on with higher dimensional models to try to understand this procedure better.

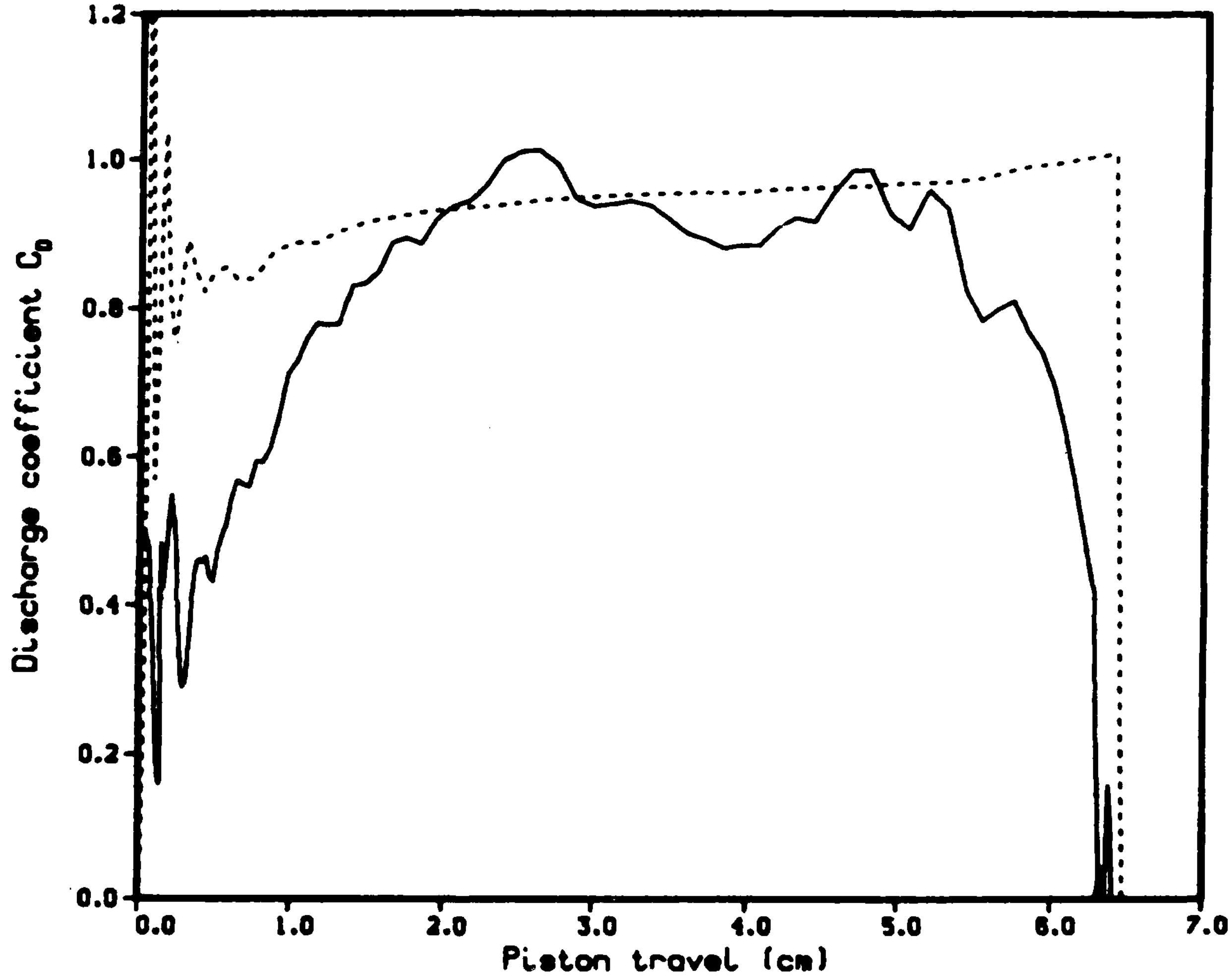

Figure 18. Discharge Coefficient into Combustion Chamber; Round 8 (line). Transient Model Discharge Coefficient into Combustion Chamber (dot)

IX. CONCLUSIONS

We have demonstrated the change in the discharge coefficient during the firing cycle and the accumulation of liquid in the combustion chamber. Both of these effects are important in resolving the details of the firing cycle. But if the proper maximum chamber pressure is achieved, the effect on muzzle velocity is relatively minor.

Attempts have been made to predict the injection into the combustion chamber, instead of using experimentally derived values. While the behavior can be qualitatively predicted, the quantitative behavior cannot be reproduced.

REFERENCES

1. Coffee, T.P., "The Analysis of Experimental Measurements for Liquid Regenerative Guns," Technical Report BRL-TR-2731, May 1986.

2. Pagan, G. and Izod, D.C.A., "Regenerative Liquid Propellant Gun Modelling," Proceedings of the Seventh International Symposium on Ballistics, The Hague, The Netherlands, April 1983.

3. Cushman, P.G., "Regenerative Liquid Propellant Gun Simulation User's Manual," GE Report 84-POD-004, December 1983.

4. Gough, P.S., "A Model of the Interior Ballistics of Hybrid Liquid-Propellant Guns," Final Report, Contract DAAK11-82-C-1054, PGA-TR-83-4, September 1983.

5. Coffee, T.P., "A Lumped Parameter Code for Regenerative Liquid Propellant Guns," BRL-TR-2703, December 1985.

6. Reever, K. P., "Operating Manual and Final Test Report for 30-mm BRL Regenerative Liquid Propellant Test Fixture," General Electric Contract Report No. DAAK 11-83-C-0007.

7. Knapton, J.D., Watson, C., and DeSpirito, J., "Test Data from a Regenerative Sheet Injector Type of Liquid Propellant Gun," 22nd JANNAF Combustion Meeting, October 1985.

8. Watson, C., private communication, 1986.

9. Freedman, E., private communication, 1986.

10. Constantino, M., "The High Pressure Equation of State of LGP 1845 and LGP 1846 (U)," UCRL-93985 preprint, Aug. 1986. Submitted to the 1986 JANNAF Propulsion Meeting.

11. McBratney, W.F., "Windowed Chamber Investigation of the Burning Rate of Liquid Monopropellants for Guns," ARBRL-MR-03018, April 1980.

12. McBratney, W.F., "Burning Rate Data, LGP 1843," ARBRL-MR-03128, August 1981.

13. Pasko, W., private communication, 1986.

LIST OF SYMBOLS

A_1	area of liquid reservoir, cm^2
A_3	area of combustion chamber, cm^2
A_4	area of the gun tube, cm^2
A_g	area of the grease dyke, cm^2
A_h	area of the piston hole, cm^2
A_v	vent area between piston and bolt, cm^2
b	covolume of the gas, cm^3/g
c_v	specific heat at constant volume, joules/g-K
c_p	specific heat at constant pressure, joules/g-K
C_D	discharge coefficient into the combustion chamber
C_T	discharge coefficient into the gun tube
d_S	Sauter mean diameter for the droplet distribution, cm
E_{K4}	kinetic energy of the fluid in the tube, joules
E_{34}	total energy in the combustion chamber/gun tube, joules
E_{ps}	kinetic energy of the piston, joules
E_{pj}	kinetic energy of the projectile, joules
E_t	total energy in the gun system, joules
e_1	chemical energy of the liquid, joules/g
e_3	internal energy of the gas in the chamber, joules/g
e_4	internal energy of the gas in the tube, joules/g
g_o	conversion constant, 10^7 g/s^2-cm-MPa
K_1	bulk modulus of the liquid at zero pressure, MPa
K_2	derivative of the bulk modulus
M_{L3}	mass of the liquid in the combustion chamber, g
M_{G3}	mass of the gas in the combustion chamber, g
M_3	total mass in the combustion chamber, g

M_{L4}	mass of the liquid in the gun tube, g
M_{G4}	mass of the gas in the gun tube, g
M_4	total mass in the gun tube, g
M_{L34}	mass of the liquid in the combustion chamber/gun tube, g
M_{G34}	mass of the gas in the combustion chamber/gun tube, g
M_{34}	total mass in the combustion chamber/gun tube, g
M_{ps}	mass of the piston, g
M_{pj}	mass of the projectile, g
P_1	pressure in the liquid reservoir, MPa
P_3	pressure in the combustion chamber, MPa
P_4	average pressure in the gun tube, MPa
P_{th}	pressure at the gun tube throat, MPa
S_{max}	maximum piston travel, cm
T_3	temperature in the combustion chamber, K
T_4	average temperature in the gun tube, K
T_{th}	temperature at the gun tube throat, K
V_1	volume of the liquid reservoir, cm^3
V_3	volume of the combustion chamber, cm^3
V_{L3}	volume of the liquid in the combustion chamber, cm^3
V_{G3}	volume of the gas in the combustion chamber, cm^3
V_4	volume of the gun tube, cm^3
V_{L4}	volume of the liquid in the gun tube, cm^3
V_{G4}	volume of the gas in the gun tube, cm^3
V_{L34}	volume of the liquid in the combustion chamber/gun tube, cm^3
V_{G34}	volume of the gas in the combustion chamber/gun tube, cm^3
V_{34}	total volume of the combustion chamber/gun tube, cm^3
v_{ps}	velocity of the piston, cm/s

v_{pj}	velocity of the projectile, cm/s
v_3	injection velocity of the fluid into the chamber, cm/s
γ	ratio of specific heats
ρ_o	density of the liquid at atmospheric pressure, g/cm^3
ρ_1	density of the liquid in the reservoir, g/cm^3
ρ_{L3}	density of the liquid in the combustion chamber, g/cm^3
ρ_{G3}	density of the gas in the combustion chamber, g/cm^3
ρ_{L4}	density of the liquid in the gun tube, g/cm^3
ρ_{G4}	density of the gas in the gun tube, g/cm^3

APPENDIX A

APPENDIX A

The properties of the fluid in the combustion chamber/gun tube are found using conservation of mass and energy. At any given time, the mass of the liquid remaining in the reservoir is known. Assuming the reservoir liquid is isothermal, we also know its chemical energy. Our basic assumption is that the system is adiabatic. That is, all loss terms are ignored (such as heat loss to the gun tube). So we can compute the total mass and energy of the combustion chamber/gun tube. A secondary assumption is that the liquid combusts completely. That is, when the liquid burns, it turns immediately into final products and releases all its chemical energy.

The set of equations is total energy:

$$E_{34} = e_1 (M_{L3} + M_{L4}) + e_3 M_{G3} + e_4 M_{G4} \tag{A1}$$

total mass:

$$M_{34} = M_{L3} + M_{G3} + M_{L4} + M_{G4} \tag{A2}$$

volumes:

$$V_3 = V_{L3} + V_{G3} \tag{A3}$$

$$V_4 = V_{L4} + V_{G4} \tag{A4}$$

internal energy (Noble-Able equation):

$$e_3 = c_v\ T_3 = p_3\ (1 - b\ \rho_{G3})/[\rho_{G3}\ (\gamma - 1)] \tag{A5}$$

$$e_4 = c_v\ T_4 = p_4\ (1-b\ \rho_{G4})/[\rho_{G4}(\gamma - 1)] \tag{A6}$$

average gun tube pressure (Lagrange distribution):

$$p_4 = p_{th}\ [1 + M_4/(3M_{pj})]/[1 + M_4/(2M_{pj})] \tag{A7}$$

and densities:

$$\rho_{L3} = M_{L3}/V_{L3} \tag{A8}$$

$$\rho_{G3} = M_{G3}/V_{G3} \tag{A9}$$

$$\rho_{L4} = M_{L4}/V_{L4} \tag{A10}$$

$$\rho_{G4} = M_{G4}/V_{G4} \tag{A11}$$

The thirteen unknowns are p_4, M_{L3}, M_{G3}, M_{L4}, M_{G4}, V_{L3}, V_{G3}, V_{L4}, V_{G4}, ρ_{L3}, ρ_{G3}, ρ_{L4}, and ρ_{G4}.To solve the equations, I assume that the liquid is evenly distributed in the combustion chamber/gun tube, that is:

$$M_{L4} = M_{L3}\ V_4/V_3 \tag{A12}$$

Finally, I assume that the internal energy of the gas is the same in the combustion chamber and the gun tube, that is:

$$e_3 = e_4 \tag{A13}$$

Since the specific heat is taken to be constant, this means that the temperature is the same. This is consistent with Bernoulli flow, but not with isentropic flow. However, in running the gun code, the temperature difference between the combustion chamber and the throat is usually no larger than 100K. Until temperature measurements are made, this is the best assumption that I can make.

The above equations are actually solved using an iterative procedure. To start with, the mass terms are estimated. The total mass M_{34} is known. I assume that the fraction of the total mass for each mass term is the same as for the previous time step. For time zero, there is no liquid accumulation, so the starting point is easily calculated. Then the following equations are solved in the given order.

Kinetic energy of the gas in the gun tube (Lagrange distribution):

$$E_{K4} = 0.5\ M_4\ v_{pj}^{\ 2} /\ 3g_o \tag{A14}$$

total energy in the combustion chamber/gun tube:

$$E_{34} = E_t - e_1\ M_1 - E_{ps} - E_{pj} - E_{K4} \tag{A15}$$

internal energy of the gas

$$e_3 = e_4 = [E_{34} - e_1\ M_{L34}] /\ M_{G34} \tag{A16}$$

average gun tube pressure

$$P_4 = P_{th} [1 + M_4/3\ M_{pj}]/ [1 + M_4/2\ M_{pj}] \tag{A17}$$

average gun tube liquid density:

$$\rho_{L4} = \rho_o \left[\frac{K_2}{K_1} P_4 + 1\right]^{1/K_2} \tag{A18}$$

gas densities:

$$\rho_{G3} = P_3/[e_3 (\gamma - 1) + P_3 b] \tag{A19}$$

$$\rho_{G4} = P_4/[e_4 (\gamma - 1) + P_4 b] \tag{A20}$$

volumes:

$$V_{L3} = M_{L3}/\rho_{L3} \tag{A21}$$

$$V_{L4} = M_{L4}/\rho_{L4} \tag{A22}$$

$$V_{G3} = V_3 - V_{L3} \tag{A23}$$

$$V_{G4} = V_4 - V_{L4} \tag{A24}$$

and finally new values for the masses:

$$M_{G3} = \rho_{G3} V_{G3} \tag{A25}$$

$$M_{G4} = \rho_{G4} V_{G4} \tag{A26}$$

$$M_{L3} = M_{L34} V_3 / V_{34} \tag{A27}$$

$$M_{L4} = M_{L34} V_4 / V_{34} \tag{A28}$$

The process is repeated until convergence is obtained. Since for any time step only minor changes occur, *this* has *not* been observed to take more than a maximum of twenty iterations. After going through all the data points in order, all the quantities needed to compute the mass accumulation and the discharge coeffici nt into the gun tube are available.

DISTRIBUTION LIST

No. of Copies	Organization
12	Commander Defense Technical Info Center ATTN: DTIC-DDA Cameron Station Alexandria, VA 22304-6145
1	Director Defense Advanced Research Projects Agency ATTN: H. Fair 1400 Wilson Boulevard Arlington, VA 22209
1	HQDA DAMA-ART-M Washington, DC 20310
1	Commander US Army Materiel Command ATTN: AMCDRA-ST 5001 Eisenhower Avenue Alexandria, VA 22333-0001
13	Commander Armament R&D Center US Army AMCCOM ATTN: SMCAR-TSS SMCAR-TDC SMCAR-SCA, B. Brodman R. Yalamanchili SMCAR-AEE-B, D. Downs A. Beardell SMCAR-LCE, N. Slagg SMCAR-LCS, W. Quine A. Bracuti J. Lannon SMCAR-FSS-A, R. Price L. Frauen SMCAR-FSA-S, H. Liberman Picatinny Arsenal, NJ 07806-5000
3	Director Benet Weapons Laboratory Armament R&D Center US Army AMCCOM ATTN: SMCAR-LCB-TL E. Conroy A. Graham Watervliet, NY 12189
1	Commander US Army Armament, Munitions and Chemical Command ATTN: SMCAR-ESP-L Rock Island, IL 61299-7300
1	Commander US Army Aviation Research and Development Command ATTN: AMSAV-E 4300 Goodfellow Blvd. St. Louis, MO 63120
1	Commander Materials Technology Lab US Army Laboratory Cmd ATTN: SLCMT-MCM-SB M. Levy Watertown, MA 02172-0001
1	Director US Army Air Mobility Rsch. and Development Lab. Ames Research Center Moffett Field, CA 94035
1	Commander US Army Communications Electronics Command ATTN: AMSEL-ED Fort Monmouth, NJ 07703
1	Commander ERADCOM Technical Library ATTN: STET-L Ft. Monmouth, NJ 07703-5301

DISTRIBUTION LIST

No. of Copies	Organization	No. of Copies	Organization
1	Commander US Army Harry Diamond Labs ATTN: DELHD-TA-L 2800 Powder Mill Rd Adelphi, MD 20783	1	Commander Armament Rsch & Dev Ctr US Army Armament, Munitions and Chemical Command ATTN: SMCAR-CCS-C, T Hung Picatinny Arsenal, NJ 07806-5000
1	Commander US Army Missile Command Rsch, Dev, & Engr Ctr ATTN: AMSMI-RD Redstone Arsenal, AL 35898	1	Commandant US Army Field Artillery School ATTN: ATSF-CMW Ft Sill, OK 73503
1	Commander US Army Missile & Space Intelligence Center ATTN: AIAMS-YDL Redstone Arsenal, AL 35898-5500	1	Commandant US Army Armor Center ATTN: ATSB-CD-MLD Ft Knox, KY 40121
1	Commander US Army Belvoir R&D Ctr ATTN: STRBE-WC Tech Library (Vault) B-315 Fort Belvoir, VA 22060-5606	1	Commander US Army Development and Employment Agency ATTN: MODE-TED-SAB Fort Lewis, WA 98433
1	Commander US Army Tank Automotive Cmd ATTN: AMSTA-TSL Warren, MI 48397-5000	1	Commander Naval Surface Weapons Center ATTN: D.A. Wilson, Code G31 Dahlgren, VA 22448-5000
1	Commander US Army Research Office ATTN: Tech Library P.O. Box 12211 Research Triangle Park,NC 27709-2211	1	Commander Naval Surface Weapons Center ATTN: Code G33, J. East Dahlgren, VA 22448-5000
1	Director US Army TRADOC Systems Analysis Activity ATTN: ATAA-SL White Sands Missile Range NM 88002	2	Commander US Naval Surface Weapons Ctr. ATTN: O. Dengel K. Thorsted Silver Spring, MD 20902-5000
1	Commandant US Army Infantry School ATTN: ATSH-CD-CSO-OR Fort Benning, GA 31905	1	Commander Naval Weapons Center China Lake, CA 93555-6001
		1	Commander Naval Ordnance Station ATTN: C. Dale Code 5251 Indian Head, MD 20640

DISTRIBUTION LIST

No. of Copies	Organization
1	Superintendent Naval Postgraduate School Dept of Mechanical Eng. ATTN: Code 1424, Library Monterey, CA 93943
1	AFWL/SUL Kirtland AFB, NW 87117
1	Air Force Armament Lab ATTN: AFATL/DLODL Eglin, AFB, FL 32542-5000
1	AFOSR/NA (L. Caveny) Bldg. 410 Bolling AFB, DC 20332
1	Commandant USAFAS ATTN: ATSF-TSM-CN Ft Sill, OK 73503-5600
1	US Bureau of Mines ATTN: R.A. Watson 4800 Forbes Street Pittsburgh, PA 15213
1	Director Jet Propulsion Lab ATTN: Tech Libr 4800 Oak Grove Drive Pasadena, CA 91109
2	Director National Aeronautics and Space Administration ATTN: MS-603, Tech Lib MS-86, Dr. Povinelli 21000 Brookpark Road Lewis Research Center Cleveland, OH 44135
1	Director National Aeronautics and Space Administration Manned Spacecraft Center Houston, TX 77058
10	Central Intelligence Agency Office of Central Reference Dissemination Branch Room GE-47 HQS Washington, DC 20502
1	Central Intelligence Agency ATTN: Joseph E. Backofen HQ Room 5F22 Washington, DC 20505
4	Bell Aerospace Textron ATTN: F. Boorady K. Berman A.J. Friona J. Rockenfeller Post Office Box One Buffalo, NY 14240
1	Calspan Corporation ATTN: Tech Library P.O. Box 400 Buffalo, NY 14225
7	General Electric Ord. Sys Dpt ATTN: J. Mandzy, OP43-220 R.E. Mayer H. West M. Bulman R. Pate I. Magoon J. Scudiere 100 Plastics Avenue Pittsfield, MA 01201-3698
1	General Electric Company Armanent Systems Department ATTN: D. Maher Burlington, VT 05401
1	IITRI ATTN: Library 10 W. 35th St. Chicago, IL 60616
1	Olin Chemicals Research ATTN: David Gavin P.O. Box 586 Chesire, CT 06410-0586

DISTRIBUTION LIST

No. of Copies	Organization
2	Olin Corporation ATTN: Victor A. Corso Dr. Ronald L. Dotson P.O. Box 30-9644 New Haven, CT 06536
1	Paul Gough Associates ATTN: Paul Gough PO Box 1614 Portsmouth, NH 03801
1	Safety Consulting Engr ATTN: Mr. C. James Dahn 5240 Pearl St. Rosemont, IL 60018
1	Science Applications, Inc. ATTN: R. Edelman 23146 Cumorah Crest Woodland Hills, CA 91364
1	Sunstrand Aviation Operations ATTN: Dr. Owen Briles P.O. Box 7002 Rockford, IL 61125
1	Veritay Technology, Inc. ATTN: E. B. Fisher 4845 Millersport Highway, P.O. Box 305 East Amherst, NY 14051-0305
1	Director Applied Physics Laboratory The Johns Hopkins Univ. Johns Hopkins Road Laurel, Md 20707
2	Director Chemical Propulsion Info Agency The Johns Hopkins Univ. ATTN: T. Christian Tech Lib Johns Hopkins Road Laurel, MD 20707

No. of Copies	Organization
2	University of Delaware Department of Chemistry ATTN: Mr. James Cronin Professor Thomas Brill Newark, DE 19711
1	U. of ILLinois at Chicago ATTN: Professor Sohail Murad Dept of Chemical Eng Box 4348 Chicago, IL 60680
1	U. of Maryland at College Park ATTN: Professor Franz Kasler Department of Chemistry College Park, MD 20742
1	U. of Missouri at Columbia ATTN: Professor R. Thompson Department of Chemistry Columbia, MO 65211
1	U. of Michigan ATTN: Prof. Gerard M. Faeth Department of Aerospace Engineering Ann Arbor, MI 48109-3796
1	U. of Missouri at Columbia ATTN: Professor F. K. Ross Research Reactor Columbia, MO 65211
1	U. of Missouri at Kansas City Department of Physics ATTN: Prof. R.D. Murphy 1110 East 48th Street Kansas City, MO 64110-2499
1	Pennsylvania State University Dept. of Mechnical Eng ATTN: K. Kuo University Park, PA 16802

DISTRIBUTION LIST

No. of Copies	Organization	No. of Copies	Organization
2	Princeton Combustion Rsch Laboratories, Inc. ATTN: N.A. Messina M. Summerfield 475 US Highway One North Monmouth Junction, NJ 08852		
1	University of Arkansas Department of Chemical Engineering ATTN: J. Havens 227 Engineering Building Fayetteville, AR 72701		
	Aberdeen Proving Ground		
	Dir, USAMSAA ATTN: AMXSY-D AMXSY-MP, H. Cohen		
	Cdr, USATECOM ATTN: AMSTE-TO-F		
	CDR, CRDEC, AMCCOM ATTN: SMCCR-RSP-A SMCCR-MU SMCCR-SPS-IL		

USER EVALUATION SHEET/CHANGE OF ADDRESS

This Laboratory undertakes a continuing effort to improve the quality of the reports it publishes. Your comments/answers to the items/questions below will aid us in our efforts.

1. BRL Report Number ______________ Date of Report ______________

2. Date Report Received ______________

3. Does this report satisfy a need? (Comment on purpose, related project, or other area of interest for which the report will be used.) ______________

4. How specifically, is the report being used? (Information source, design data, procedure, source of ideas, etc.) ______________

5. Has the information in this report led to any quantitative savings as far as man-hours or dollars saved, operating costs avoided or efficiencies achieved, etc? If so, please elaborate. ______________

6. General Comments. What do you think should be changed to improve future reports? (Indicate changes to organization, technical content, format, etc.)

CURRENT ADDRESS

Name ______________

Organization ______________

Address ______________

City, State, Zip ______________

7. If indicating a Change of Address or Address Correction, please provide the New or Correct Address in Block 6 above and the Old or Incorrect address below.

OLD ADDRESS

Name ______________

Organization ______________

Address ______________

City, State, Zip ______________

(Remove this sheet, fold as indicated, staple or tape closed, and mail.)

— — — — — — — — — — FOLD HERE — — — — — — — — — — — —

Director
US Army Ballistic Research Laboratory
ATTN: DRXBR-OD-ST
Aberdeen Proving Ground, MD 21005-5066

NO POSTAGE
NECESSARY
IF MAILED
IN THE
UNITED STATES

OFFICIAL BUSINESS
PENALTY FOR PRIVATE USE, $300

BUSINESS REPLY MAIL
FIRST CLASS PERMIT NO 12062 WASHINGTON, DC

POSTAGE WILL BE PAID BY DEPARTMENT OF THE ARMY

Director
US Army Ballistic Research Laboratory
ATTN: DRXBR-OD-ST
Aberdeen Proving Ground, MD 21005-9989

— — — — — — — — — — FOLD HERE — — — — — — — — — — — —

END
FEb.
1988
DTIC